NASA TECHNICAL NOTE

NASA TN D-5117

OPTIMAL THREE DIMENSIONAL LAUNCH VEHICLE TRAJECTORIES WITH ATTITUDE AND ATTITUDE RATE CONSTRAINTS

by Fred Teren and Omer F. Spurlock

Lewis Research Center
Cleveland, Ohio

NATIONAL AERONAUTICS AND SPACE ADMINISTRATION • WASHINGTON, D. C. • MARCH 1969

OPTIMAL THREE DIMENSIONAL LAUNCH VEHICLE TRAJECTORIES WITH ATTITUDE AND ATTITUDE RATE CONSTRAINTS

By Fred Teren and Omer F. Spurlock

Lewis Research Center
Cleveland, Ohio

NATIONAL AERONAUTICS AND SPACE ADMINISTRATION

For sale by the Clearinghouse for Federal Scientific and Technical Information
Springfield, Virginia 22151 – CFSTI price $3.00

ABSTRACT

Equations are derived for maximizing payload capability for nonplanar boost trajectories arising from range safety considerations. The assumed range safety constraints are satisfied by requiring a fixed vehicle azimuth heading during the initial part of the trajectory. This azimuth (attitude) constraint is removed as soon as certain land areas have been avoided. An attitude rate limit is also imposed to prevent discontinuous attitude changes. The calculus of variations is used to formulate and solve the mathematical problem. A simplified method is also presented for obtaining the auxiliary variational terminal conditions associated with free end conditions. Sample results are presented for sun-synchronous and planetary missions.

OPTIMAL THREE DIMENSIONAL LAUNCH VEHICLE TRAJECTORIES WITH ATTITUDE AND ATTITUDE RATE CONSTRAINTS

by Fred Teren and Omer F. Spurlock

Lewis Research Center

SUMMARY

Equations are derived for maximizing payload capability for nonplanar boost trajectories arising from range safety considerations. The assumed range safety constraints are satisfied by requiring a fixed vehicle azimuth heading during the initial part of the trajectory. This azimuth (attitude) constraint is removed as soon as certain land areas have been avoided. An attitude rate limit is also imposed to prevent discontinuous attitude changes. The calculus of variations is used to formulate and solve the mathematical problem. A simplified method is also presented for obtaining the auxiliary variational terminal conditions associated with free end conditions. Sample results are presented for sun-synchronous and planetary missions.

INTRODUCTION

Injection conditions for most earth orbital and planetary missions are achieved by using essentially planar steering throughout the entire launch vehicle-powered flight trajectory. A planar trajectory results from selecting the launch azimuth heading which gives the desired orbital inclination or declination and right ascension of the outgoing asymptote without yaw steering. However, range safety instantaneous impact point (IIP) restrictions sometimes do not permit the use of the launch azimuth required for a planar trajectory. In such cases, the required injection conditions may be achieved by employing a nonplanar trajectory and steering the vehicle so that the probablility of impacting land masses is eliminated or at least minimized.

The rigorous optimization of trajectories with IIP constraints requires a detailed specification of the IIP restrictions. These restrictions must then be formulated mathematically and included along with the vehicle equations of motion and mission constraints and requirements. This problem can be solved by using the calculus of variations. How-

ever, the IIP restrictions result in an extremely tedious mathematical formulation. Therefore, a simplified solution procedure is presented in this report. A launch azimuth heading is chosen which allows the initial portion of the trajectory to avoid all land masses. The thrust direction is restricted to be parallel to the launch azimuth plane (the direction within the plane is optimized) until the IIP has passed the protected land masses. Then, the planar steering constraint is removed and optimal three-dimensional steering is used to satisfy the required injection conditions at powered flight termination.

At the switching point between planar and unrestricted steering, the optimum trajectory requires a discontinuous change in vehicle attitude, if no attitude rate limits are imposed. Since a discontinous attitude change is not physically possible, an attitude rate limit is added to the problem formulation.

The calculus of variations has been used extensively in the past to solve both two- and three-dimensional trajectory problems. Reference 1 derives equations for optimal two-dimensional ascent trajectories and also includes equations for optimizing stage propellant loadings. Equations for optimal three-dimensional interplanetary trajectories are derived in reference 2. Equations have been developed by Johnson and Winfield (ref. 3) for rate limited optimal trajectories. In that report, the rate limit problem arose because of constraints on initial and/or final thrust direction. Consequently, the rate-limited phases (referred to as regular arcs) occur at the beginning and/or end of the trajectory. Intermediate attitude rates are used throughout the rest of the trajectory. These intermediate attitude rates result from the existence of singular arcs in the optimal trajectory. The equations are derived by using the maximum principle, and a possible solution procedure is discussed. However, no numerical examples are solved.

The present report extends the analysis of reference 3 to include constraints on vehicle attitude, as well as attitude rate. Also, the problem solution requires regular arcs in the center, rather than at the ends, of the trajectory. The calculus of variations is used to obtain the mathematical problem formulation. A simplified method is also presented for deriving the auxiliary variational boundary conditions associated with free trajectory injection conditions.

In order to illustrate the use of the equations, solutions are presented for two typical missions which require nonplanar trajectories of the type described. An Atlas-Centaur launch vehicle is assumed for both of these missions with an Eastern Test Range (ETR) launch. The first mission is a high altitude (1110 km) sun-synchronous orbit, with a required orbital inclination of 99.9°. The second mission presented is a typical Mars or Venus probe with a declination of the outgoing asymptote of -45°.

ANALYSIS

The problem to be solved is to determine the optimal thrust direction profile for a

trajectory satisfying certain boundary conditions. The thrust direction is constrained to lie in a fixed inertial plane during the initial part of the trajectory; later, the thrust direction is completely free in three dimensions. However, the attitude rate is constrained to be less than or equal to a prespecified limit throughout the variational portion of the trajectory. At the transition point between the constrained and unconstrained attitude portions, a discontinuity in thrust direction occurs in the optimum trajectory if no attitude rate limit is imposed. However, a maximum turning rate is specified in the present problem so that the vehicle will rotate at the maximum rate (regular arc) in this region. The boundary value discussion presented in this report does not consider the possibility of regular arcs occurring in other regions of the trajectory. Generally, the maximum turning rate is large enough so that additional regular arcs are not required. If additional regular arcs do occur, the boundary value problem must be altered accordingly.

Problems of this type can be formulated as a Bolza problem (ref. 4). Specifically, the functional to be minimized is written as:

$$J = g + \int_{t_0}^{t_f} F \, dt \tag{1a}$$

where

$$F = \bar{\lambda} \cdot \bar{b}_1 + \bar{\mu} \cdot \bar{b}_2 + \bar{\sigma} \cdot \bar{b}_3 + \gamma b_4 + \rho b_5 \tag{1b}$$

and

$$g = t_f \tag{1c}$$

subject to the following constraints:

$$\bar{b}_1 = \dot{\bar{v}} + \frac{Gm}{r^3}\bar{r} - a\hat{f} = \bar{0} \tag{2a}$$

$$\bar{b}_2 = \dot{\bar{r}} - \bar{v} = \bar{0} \tag{2b}$$

$$\bar{b}_3 = \dot{\hat{f}} - \bar{\omega} \times \hat{f} = \bar{0} \tag{2c}$$

$$b_4 = \bar{\omega} \cdot \bar{\omega} - \omega_m^2 = 0 \tag{2d}$$

$$b_5 = (\bar{\omega} \times \hat{f}) \cdot \hat{n} = 0 \tag{2e}$$

All symbols used herein are defined in appendix A.

Equations (2a) and (2b) are the vehicle equations of motion written in three-dimensional rectangular coordinates. The thrust acceleration profile, a, is assumed to be a definite function of time. The unit vector $\hat{f}$ defines the thrust direction. Equation (2c) determines the rotation rate $\dot{\hat{f}}$ as a rotation of $\hat{f}$ about the vector $\overline{\omega}$. Since $\dot{\hat{f}}$ is perpendicular to $\hat{f}$, the magnitude of $\hat{f}$ is constant (as required) and is set equal to unity as an initial condition. The optimum vehicle turning vector, $\overline{\omega}$, will be determined by the variational analysis. However, the magnitude of $\dot{\hat{f}}$ must not exceed the maximum turning rate, ω_m. This constraint is satisfied by equation (2d), which states that the magnitude of $\overline{\omega}$ is equal to ω_m. From equation (2c), the magnitude of $\dot{\hat{f}}$ is equal to ω_m if $\overline{\omega}$ is perpendicular to $\hat{f}$; otherwise, the rotation rate is less than ω_m. Since no restriction has been placed on the direction of $\overline{\omega}$, equations (2c) and (2d) are equivalent to an inequality constraint on $\dot{\hat{f}}$.

Equation (2e) is used only when the planar attitude constraint is in effect. (The unit vector $\hat{n}$ is the normal to the required thrusting plane.) When the attitude is unconstrained, ρ is set equal to zero. Equation (2e) requires the component of $\dot{\hat{f}}$ along $\hat{n}$ to be zero (i.e., $\hat{f} \cdot \hat{n}$ is constant). The value of $\hat{f} \cdot \hat{n}$ is set equal to zero as an initial condition.

The variables $\overline{\lambda}$, $\overline{\mu}$, $\overline{\sigma}$, γ, and ρ are undetermined Lagrange multipliers which are functions of time since the constraint equations must be satisfied at all points of the trajectory. The Euler-Lagrange equations for this problem (ref. 4) are

$$\dot{\overline{\lambda}} + \overline{\mu} = \overline{0} \tag{3a}$$

$$\dot{\overline{\mu}} - \frac{Gm}{r^3}\overline{\lambda} + 3\frac{Gm}{r^5}(\overline{\lambda} \cdot \overline{r})\overline{r} = \overline{0} \tag{3b}$$

$$\dot{\overline{\sigma}} + a\overline{\lambda} + \overline{\sigma} \times \overline{\omega} + \rho\overline{\omega} \times \hat{n} = \overline{0} \tag{3c}$$

$$2\gamma\overline{\omega} - \hat{f} \times \overline{\sigma} + \rho\dot{\hat{f}} \times \hat{n} = \overline{0} \tag{3d}$$

The turning rates for the planar and unconstrained attitude cases must be considered separately. For the unconstrained attitude case ($\rho = 0$), combining equations (3d) and (2d) results in

$$\omega = \pm\omega_m \frac{\hat{f} \times \overline{\sigma}}{|\hat{f} \times \overline{\sigma}|} \tag{4}$$

Thus, the optimal turning rate has been determined, except for sign. The proper choice of sign will be determined later. Since $\overline{\omega} \cdot \hat{f} = 0$ (from eq. (4)), the maximum turning

rate (regular arc) is always used, unless $\hat{f} \times \bar{\sigma} = \bar{0}$ in which case $\bar{\omega}$ is indeterminate. It will be shown later that $\hat{f} \times \bar{\sigma} \equiv \bar{0}$ corresponds to the singular arc.

For the planar attitude case, equations (2d) and (3d) give:

$$\omega = \pm\omega_m \left[\frac{\hat{f} \times \bar{\sigma} - \rho \hat{f} \times \hat{n}}{\left| \hat{f} \times \bar{\sigma} - \rho \hat{f} \times \hat{n} \right|} \right]$$

The value of ρ is determined by combining equations (2e) and (3d). This procedure results in:

$$\rho = (\hat{f} \times \bar{\sigma}) \cdot (\hat{f} \times \hat{n})$$

If $\hat{f} \times \bar{\sigma}$ is expressed in the orthonormal $\hat{f}$, $\hat{n}$, $\hat{f} \times \hat{n}$ coordinate system,

$$\hat{f} \times \bar{\sigma} = \left[(\hat{f} \times \bar{\sigma}) \cdot \hat{f} \right] \hat{f} + \left[(\hat{f} \times \bar{\sigma}) \cdot \hat{n} \right] \hat{n} + \left[(\hat{f} \times \bar{\sigma}) \cdot (\hat{f} \times \hat{n}) \right] \hat{f} \times \hat{n}$$

and since $(\hat{f} \times \sigma) \cdot \hat{f} = 0$,

$$\hat{f} \times \bar{\sigma} - \left[(\hat{f} \times \bar{\sigma}) \cdot (\hat{f} \times \hat{n}) \right] \hat{f} \times \hat{n} = \left[(\hat{f} \times \bar{\sigma}) \cdot \hat{n} \right] \hat{n}$$

or

$$\hat{f} \times \bar{\sigma} - \rho \hat{f} \times \hat{n} = \left[(\hat{f} \times \bar{\sigma}) \cdot \hat{n} \right] \hat{n}$$

Therefore,

$$\bar{\omega} = \pm\omega_m \operatorname{sign} \left[(\hat{f} \times \bar{\sigma}) \cdot \hat{n} \right] \hat{n} \tag{5}$$

Since $\bar{\omega} \cdot \hat{f} = 0$, the maximum turning rate is used on the regular planar arc, just as on the regular unconstrained arc. The singular planar arc occurs when $(\hat{f} \times \bar{\sigma}) \cdot \hat{n} = 0$.

Weierstrass Condition

The uncertainty in sign in equations (4) and (5) can be resolved with the aid of the Weierstrass E-test (ref. 5), which can be stated as

$$E \geq 0 \quad \text{for a minimum}$$

where

$$E = F(x_i^*, \dot{x}_i^*) - F(x_i, \dot{x}_i) - \sum_i (\dot{x}_i^* - \dot{x}_i) \frac{\partial F}{\partial \dot{x}_i} \tag{6}$$

The x_i correspond to the minimizing values of the problem variables ($\bar{r}$, $\bar{v}$, $\hat{f}$, and $\bar{\omega}$), which differ from the x_i^* by a finite but admissible amount. For the present problem, only $\bar{\omega}$ is subject to such a variation, and equation (6) can be written explicitly as

$$E = \bar{\sigma} \cdot (\bar{\omega} - \bar{\omega}^*) \times \hat{f} \geq 0 \text{ for a minimum.}$$

Since $\bar{\omega}^* = -\bar{\omega}$, this equation becomes

$$\bar{\omega} \cdot (\bar{\sigma} \times \hat{f}) \leq 0 \tag{7}$$

for a minimum.

For the unconstrained attitude case, combining equations (4) and (7) results in

$$\pm\omega_m \frac{(\hat{f} \times \bar{\sigma}) \cdot (\bar{\sigma} \times \hat{f})}{|\hat{f} \times \bar{\sigma}|} \leq 0$$

or

$$\pm\omega_m |\hat{f} \times \bar{\sigma}| \geq 0$$

which requires that the plus sign be chosen in equation (4):

$$\bar{\omega} = \omega_m \frac{\hat{f} \times \bar{\sigma}}{|\hat{f} \times \bar{\sigma}|} \tag{8}$$

For the planar attitude case, equations (5) and (7) are combined to give:

$$\pm\omega_m \operatorname{sign}\left[(\hat{f} \times \bar{\sigma}) \cdot \hat{n}\right] \hat{n} \cdot (\bar{\sigma} \times \hat{f}) \leq 0$$

or

$$\pm\omega_m |(\hat{f} \times \bar{\sigma}) \cdot \hat{n}| \geq 0$$

Again, the plus sign must be chosen. Therefore,

$$\bar{\omega} = \omega_m \operatorname{sign}\left[(\hat{f} \times \bar{\sigma}) \cdot \hat{n}\right]\hat{n} \tag{9}$$

Singular Arcs

Singular arcs occur when the Weierstrass E-function is identically zero for some finite time interval. From equations (4) and (7), this occurs for the unconstrained attitude case when $\hat{f} \times \bar{\sigma} = \bar{0}$. If $\hat{f} \times \bar{\sigma} \equiv \bar{0}$ for some finite time, then $(d/dt)(\hat{f} \times \bar{\sigma})$ must also be zero. But from equations (2c) and (3c) (with $\rho = 0$),

$$\begin{aligned}\frac{d}{dt}(\hat{f} \times \bar{\sigma}) &= (\bar{\omega} \times \hat{f}) \times \bar{\sigma} + \hat{f} \times \left[-a\bar{\lambda} - \bar{\sigma} \times \bar{\omega}\right] \\ &= (\bar{\omega} \times \hat{f}) \times \bar{\sigma} - a\hat{f} \times \bar{\lambda} - \hat{f} \times (\bar{\sigma} \times \bar{\omega}) \\ &= -a\hat{f} \times \bar{\lambda} - \bar{\omega} \times (\bar{\sigma} \times \hat{f}) = -a\hat{f} \times \bar{\lambda} = \bar{0}\end{aligned} \tag{10}$$

which implies that

$$f = \pm \frac{\bar{\lambda}}{\lambda} \tag{11}$$

for the singular arc. This is the same solution as obtained in reference 2, where no rate limit is imposed. It is shown in reference 2 that the Weierstrass E-test requires that the plus sign be chosen in equation (11). Therefore,

$$f = \frac{\bar{\lambda}}{\lambda} \tag{12}$$

is the singular solution, which takes effect when equation (12) and $\hat{f} \times \bar{\sigma} = \bar{0}$ are satisfied simultaneously.

For the planar attitude case, the singular arc and corresponding indeterminacy in $\bar{\omega}$ occur when $(\hat{f} \times \bar{\sigma}) \cdot \hat{n} \equiv 0$ (eq. (9)). The required thrust direction for the singular arc is obtained from

$$\frac{d}{dt}(\hat{f} \times \bar{\sigma}) \cdot \hat{n} = (\bar{\omega} \times \hat{f}) \times \bar{\sigma} \cdot \hat{n} + \hat{f} \times \left[-a\bar{\lambda} - \bar{\sigma} \times \bar{\omega} - \rho\bar{\omega} \times \hat{n}\right] \cdot \hat{n}$$

$$= (\bar{\omega} \times \hat{f}) \times \bar{\sigma} \cdot \hat{n} - a\hat{f} \times \bar{\lambda} \cdot \hat{n} - \hat{f} \times (\bar{\sigma} \times \bar{\omega}) \cdot \hat{n} - \rho\hat{f} \times (\bar{\omega} \times \hat{n}) \cdot \hat{n}$$

$$= -a(\hat{f} \times \bar{\lambda}) \cdot \hat{n} = 0 \tag{13}$$

Since $\hat{f}$ is normal to $\hat{n}$ and $\bar{\lambda} \times \hat{n}$, $\hat{f}$ may be written

$$\hat{f} = \pm \frac{\hat{n} \times (\bar{\lambda} \times \hat{n})}{|\bar{\lambda} \times \hat{n}|}$$

or

$$\hat{f} = \frac{\bar{\lambda} - (\bar{\lambda} \cdot \hat{n})\hat{n}}{\sqrt{\lambda^2 - (\bar{\lambda} \cdot \hat{n})^2}} \tag{14}$$

where the sign choice in equation (14) has again been made by using the Weierstrass E-test on the unrestricted rate, planar attitude solution.

Weierstrass-Erdmann Corner Condition

The boundary conditions on the Lagrange multipliers at corner points of the trajectory can be derived with the aid of the Weierstrass-Erdmann corner condition (ref. 4). This condition requires that the $\partial F/\partial \dot{x}_i$ be continuous at all corner points of the trajectory, where the x_i are the problem variables as defined earlier. For this problem, corners occur at transition points between regular and singular arcs and at the switchover point between planar and unrestricted attitude. The $\partial F/\partial \dot{x}_i$ are $\bar{\lambda}$, $\bar{\mu}$, and $\bar{\sigma}$; therefore, these variables must be continuous throughout the entire trajectory.

Trajectory Description

A list of major trajectory event times is presented in table I, along with a brief description of each event. The trajectory starts with a short vertical rise, followed by a rapid pitchover phase in the desired azimuth direction, which determines the amount of trajectory lofting during the atmospheric phase of the trajectory, as well as the vehicle

azimuth heading. The rest of the atmospheric phase (which is assumed to be terminated at booster stage burnout) is flown with a near-zero angle of attack steering program (such as described in ref. 6), in order to minimize vehicle heating and aerodynamic loads. The thrust direction is maintained perpendicular to $\hat{n}$ throughout the booster portion of the trajectory.

The variational problem begins after the sensible atmosphere has been traversed. It is assumed herein that this occurs at fixed time, position, and velocity. This implies that the magnitude of the initial pitchover is fixed. However, the degree of freedom available when the pitchover magnitude is free for optimization can also be handled by variational methods, as shown in references 1 and 6. It is also assumed that the desired initial thrust direction for the variational phase can be achieved prior to the start of this phase, so that an initial regular arc is not required. This assumption is reasonable since the attitude discontinuity at this point is generally small (see Results). The equation modifications required to handle an initial regular arc are straightforward and are described in reference 3. The thrust direction during the initial portion of the variational trajectory is constrained to be normal to $\hat{n}$, as in the booster trajectory. Thus, a singular, planar arc is used.

The initial singular, planar arc continues until a short time prior to the time at which the planar steering constraint is removed. At this point, a regular planar arc is used. This arc is not forced by saturation (i.e., the variational commanded planar turning rate does not exceed ω_m). However, a regular unconstrained arc is forced at the junction point between the planar and unconstrained portions of the trajectory, because the conditions for singularity are no longer satisfied at this point. The regular planar arc is therefore used in order to shorten the forthcoming regular unconstrained arc. In addition, the use of the regular planar arc supplies an additional degree of freedom (start time of regular planar arc) which will be needed to satisfy the boundary conditions to be discussed later. A second degree of freedom results from the fact that $\hat{f} \times \bar{\sigma}$ is not completely specified on the planar arc. Johnson and Winfield (ref. 3) discuss the fact that no additional degrees of freedom are available for regular arcs forced by saturation. However, two additional boundary conditions must be satisfied for each regular arc introduced, and these boundary conditions can only be satisfied by anticipating the forthcoming regular arc, thus allowing two additional degrees of freedom. For this reason, regular arcs forced by saturation only exist as limiting solutions.

The need for introducing a regular arc prior to saturation may be better understood by referring to a two-dimensional analogy, as illustrated in sketch a.

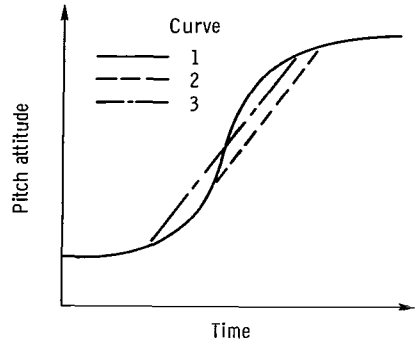

(a)

Suppose the optimal pitch attitude history for a nonrate-limited trajectory is given by curve 1. If a rate limit is introduced, the trajectory may be modified by using a regular arc starting at the saturation point (curve 2) and terminating when the attitude coincides with curve 1. The performance loss associated with curve 2 is approximately proportional to the integral of the absolute attitude difference between curves 1 and 2. This integral can be decreased by initiating the regular arc earlier (curve 3), thereby improving performance. The use of curve 3 also introduces a degree of freedom (time of regular arc initiation), which is needed to satisfy a variational boundary condition introduced because of the regular arc.

When the attitude constraint is removed, the trajectory switches from a regular planar arc to a regular unconstrained arc. This arc is then continued until the required boundary conditions for a singular arc are satisfied. At this point, a singular unconstrained arc is used and is continued until the desired end conditions are achieved. It is assumed that the final attitude is unconstrained; therefore, no final regular arc is required. Again, the equation modifications required to include a final regular arc are straightforward and are discussed in reference 3.

TRANSVERSALITY EQUATION

The relation between changes in boundary values and changes in J (eq. (1a)) is expressed by the general transversality equation (ref. 4).

$$dJ = \left[\left(F - \sum_i \dot{x}_i \frac{\partial F}{\partial \dot{x}_i}\right) dt + \sum_i \frac{\partial F}{\partial \dot{x}_i} dx_i\right]_{t_o}^{t_f} + dg = 0 \qquad (15)$$

where dJ has been set equal to zero for an optimum solution. For the present problem, dJ is evaluated to give

$$dJ = \left(C\,dt + \bar{\lambda} \cdot d\bar{v} + \bar{\mu} \cdot d\bar{r} + \bar{\sigma} \cdot d\hat{f}\right)_{t_o}^{t_f} + dt_f = 0 \tag{16}$$

where C is a constant, the first integral of the Euler-Lagrange equations (ref. 4).

$$C = \frac{Gm}{r^3}\bar{\lambda} \cdot \bar{r} - \bar{\mu} \cdot \bar{v} - a\bar{\lambda} \cdot \hat{f} - \bar{\sigma} \cdot (\bar{\omega} \times \hat{f})$$

Since it has been assumed that the initial position, velocity, and time are specified, $d\bar{r}_o = d\bar{v}_o = dt_o = 0$ and equation (16) becomes

$$\left[(C + 1)\,dt + \bar{\lambda} \cdot d\bar{v} + \bar{\mu} \cdot d\bar{r} + \bar{\sigma} \cdot d\hat{f}\right]_{t_f} - (\bar{\sigma} \cdot d\hat{f})_{t_o} = 0 \tag{17}$$

The final time is not specified so that $C = -1$ for an optimal solution. Since the Euler-Lagrange equations are homogeneous in the multipliers, $C = -1$ can be satisfied by the proper choice of multiplier scale factor. In any case, C does not appear in any of the equations used to optimize the trajectory.

The final attitude is not specified, hence $(\bar{\sigma} \cdot d\hat{f})_{t_f} = 0$ must be satisfied for an optimal solution. The allowable variation in $\hat{f}$ (perpendicular to $\hat{f}$ since $\hat{f}$ is a unit vector) is given by

$$d\hat{f} = \hat{f} \times \bar{\epsilon}$$

where $\bar{\epsilon}$ is an arbitrary vector. Therefore,

$$(\bar{\sigma} \cdot d\hat{f})_{t_f} = (\bar{\sigma} \cdot \hat{f} \times \bar{\epsilon})_{t_f} = (\bar{\sigma} \times \hat{f}) \cdot \bar{\epsilon}_{t_f} = \bar{0}$$

Since $\bar{\epsilon}$ is arbitrary,

$$(\bar{\sigma} \times \hat{f})_{t_f} = \bar{0} \tag{18}$$

is a required boundary condition.

At t_o, $\hat{f}$ has only one degree of freedom since $\hat{f} \cdot \hat{n}$ must be zero. This degree of freedom is given by

$$d\hat{f} = \alpha \hat{f} \times \hat{n}$$

where α is arbitrary. Combining this result with the last term in equation (17) gives

$$(\bar{\sigma} \times \hat{f})_{t_o} \cdot \hat{n} = 0 \tag{19}$$

for a required boundary condition. Equations (18) and (19) are also necessary conditions for singular unconstrained, and singular planar arcs, respectively.

Boundary Conditions on Position and Velocity

There exists an auxiliary variational boundary condition to be satisfied for each free trajectory end condition. By satisfying this auxiliary equation, the resulting value of the free end condition will minimize flight time. The auxiliary equations are obtained from the position and velocity terms in equation (17).

$$\bar{\lambda} \cdot d\bar{v} + \bar{\mu} \cdot d\bar{r} = 0 \tag{20}$$

Suppose the final orbit is specified in terms of arbitrary independent variables q_k

$$q_k = q_{k,d} \qquad k = 1, 2, \ldots, n \leq 6$$

If n is less than six, there are free end conditions. The set q_k is completed by additional independent variables, if necessary, to give a complete specification of the trajectory state in terms of the q_k. By expressing the components of $\bar{r}$ and $\bar{v}$ in terms of the q_k, and differentiating, equation (20) becomes

$$\sum_{k=1}^{6} \frac{\partial}{\partial q_k} (\bar{\lambda} \cdot \bar{v} + \bar{\mu} \cdot \bar{r})\, dq_k = 0$$

For each free q_k, the corresponding auxiliary boundary condition is obtained by setting

$$\frac{\partial}{\partial q_k} (\bar{\lambda} \cdot \bar{v} + \bar{\mu} \cdot \bar{r}) = 0 \tag{21}$$

This procedure, although straightforward, can be very tedious if the q's are complex functions of $\bar{r}$ and $\bar{v}$. For this reason, a simplified approach is presented for calculating the required auxiliary final conditions. With this approach, the $d\bar{r}$ and $d\bar{v}$ are interpreted as allowable variations in $\bar{r}$ and $\bar{v}$. Given a set of q_k, the allowable variations are such that all other boundary values remain constant, while the free end condition is allowed to vary. In other words, the allowable variations correspond to partial derivatives of injection position and velocity with respect to the free end conditions, as in equation (21). To illustrate the use of this procedure, the auxiliary boundary equations will be derived for the two missions considered herein.

Sun-synchronous orbit. - The required orbit conditions for the sun-synchronous orbit mission call for a circular orbit at a specified altitude (radius) with a specified orbital inclination. This is equivalent to the specification of four orbital parameters:

$$q_1 = r = r_d$$

$$q_2 = v = v_d = \sqrt{\frac{Gm}{r_d}}$$

$$q_3 = \dot{r} = \bar{v} \cdot \hat{r} = 0$$

$$q_4 = I = I_d$$

Two additional independent orbital parameters must be added to complete the set of q_k, and these additional q_k are free for optimization. The free orbital parameters may be considered to be

$$q_5 = \text{longitude of ascending node}$$

$$q_6 = \text{argument of injection latitude}$$

For free ascending node, the trajectory plane may be rotated about a vector $(\hat{z})$ pointing at the North Pole. Such a rotation changes the ascending node but leaves all other orbit parameters fixed. The allowable variations in position and velocity corersponding to this rotation are

$$d\bar{r} = \alpha\bar{r} \times \hat{z}$$

$$d\bar{v} = \alpha\bar{v} \times \hat{z}$$

where α is the arbitrary magnitude of the rotation. Combining these variations with equation (20) yields

$$\alpha(\bar{\lambda} \cdot \bar{v} \times \hat{z} + \bar{\mu} \cdot \bar{r} \times \hat{z}) = \alpha(\bar{\lambda} \times \bar{v} + \bar{\mu} \times \bar{r}) \cdot \hat{z} = 0$$

Since α is arbitrary,

$$(\bar{\lambda} \times \bar{v} + \bar{\mu} \times \bar{r}) \cdot \hat{z} = 0 \tag{22}$$

for optimum ascending node.

For free argument of injection latitude, the allowable variations in $\bar{r}$ and $\bar{v}$ result from a rotation of the trajectory about the angular momentum vector, $\bar{h}$. Hence,

$$d\bar{r} = \alpha \bar{r} \times \bar{h}$$

$$d\bar{v} = \alpha \bar{v} \times \bar{h}$$

and the auxiliary variational end condition is

$$(\bar{\lambda} \times \bar{v} + \bar{\mu} \times \bar{r}) \cdot \bar{h} = 0 \tag{23}$$

Interplanetary transfer. - The required heliocentric transfer trajectory may be specified in terms of the required hyperbolic excess velocity vector, $\bar{v}_\infty$, at Earth injection. This vector, in turn, may be specified in terms of three variables:

q_1 = injection energy (or equivalently, hyperbolic velocity magnitude)

q_2 = declination of outgoing asymptote

q_3 = right ascension of outgoing asymptote

In addition, the perigee radius of the geocentric hyperbola is specified.

$$q_4 = r_p$$

As in the sun-synchronous mission, there are two free end conditions. These correspond to

q_5 = injection true anomaly, η_I

q_6 = a free rotation of the trajectory plane about the hyperbolic excess velocity vector, $\bar{v}_\infty$

For free true anomaly, the allowable $\bar{dr}$ and $\bar{dv}$ may be obtained as changes resulting from coasting along the geocentric hyperbola at the injection point. Hence,

$$\bar{dr} = \alpha \bar{v}$$

$$\bar{dr} = \alpha \bar{G}$$

where

$$\bar{G} = -\frac{Gm}{r^3}\bar{r}$$

and α is arbitrary. Combining these variations with equation (20) results in

$$\bar{\lambda} \cdot \bar{G} + \bar{\mu} \cdot \bar{v} = 0 \tag{24}$$

for optimum true anomaly.

The auxiliary variational end condition for q_6 is obtained in a manner similar to equations (22) and (23). This equation is

$$(\bar{\lambda} \times \bar{v} + \bar{\mu} \times \bar{r}) \cdot \bar{v}_\infty = 0 \tag{25}$$

NUMERICAL ITERATION

An optimum trajectory requires the simultaneous integration of equations (2a), (2b), (2c), (3a), (3b), and (3c). As initial conditions, these equations require the initial position and velocity, as well as the multipliers $\bar{\lambda}$ and $\bar{\mu}$. Since the variational trajectory begins on a singular arc, the value of $\hat{f} \times \bar{\sigma}$ is not needed at this point. The trajectory is then uniquely specified until the transition time to the regular planar arc (t_1). This transition time, as well as the component of $\hat{f} \times \bar{\sigma}$ along $\hat{f} \times \hat{n}$ ($\hat{f} \times \bar{\sigma} \cdot \hat{n}$ must be zero while on the singular planar arc), must be supplied as initial conditions at this point. The trajectory then proceeds along the regular planar arc and into the regular unconstrained arc (at t_2). On the converged trajectory, the transition to the unconstrained singular arc (t_3) will occur when the equations for singularity are satisfied. During the iteration process, however, this transition occurs at a specified time (varied during the iteration process) and jump discontinuities in $\hat{f}$ and $\hat{f} \times \bar{\sigma}$ to the singular values are permitted. The trajectory integration then proceeds uniquely to final injection.

With the initial conditions as given above, the trajectory is uniquely specified. It remains to find the values of the unknown initial conditions which result in the trajectory satisfying the required final conditions. The initial and final conditions for the two point boundary value problem are as follows:

Unknown initial conditions:	Desired final conditions:
$\overline{\lambda}(t_o)$	Six orbital and/or auxiliary final conditions
$\overline{\mu}(t_o)$	
$(\hat{f} \times \overline{\sigma}) \cdot (\hat{f} \times \hat{n})(t_1)$	$\hat{f} \times \overline{\sigma} = \overline{0}$ (two conditions)
t_1	$\frac{\overline{\lambda}}{\lambda} \cdot \hat{f} = 1$
t_3	
t_f	$C = -1$

(26)

The boundary value problem may be simplified by using the initial value of one of the multipliers to satisfy $C = -1$. Also, the trajectory can be terminated on one of the final orbit conditions, thus eliminating t_f and one final orbit condition from the problem. The resulting iteration size is eight by eight, and the iteration variables are

Unknown initial conditions:	Desired final conditions:
Five of $\begin{cases} \overline{\lambda}(t_o) \\ \overline{\mu}(t_o) \end{cases}$	Five orbital and/or auxiliary final conditions
$(\hat{f} \times \overline{\sigma}) \cdot (\hat{f} \times \hat{n})(t_1)$	$\hat{f} \times \overline{\sigma} = \overline{0}$ (two conditions)
t_1	$\frac{\overline{\lambda}}{\lambda} \cdot \hat{f} = 1$
t_3	

(27)

The iteration process is carried out by using a multivariable Newton-Raphson method. This method is described in detail in references 1 and 6 and will not be discussed here. The only difference between the procedure described in these references and that used herein is the method of obtaining the required partial derivatives of final conditions with respect to initial conditions. In references 1 and 6 this was accomplished by using finite differences. This procedure was also attempted on the present problem. However, because of the sensitivity of the derivatives and the size of the iteration loop,

convergence was very difficult to attain. For this reason, it was decided to use integrated partial derivatives. With this procedure, convergence was easily obtained. The equations used in obtaining the required partial derivatives are presented in appendix B. A complete list of equations required to optimize the trajectory is also presented in this appendix.

Choice of Initial Conditions

In order to facilitate convergence of the two point boundary value problem, it is desirable to start the iteration with initial conditions which are as close as possible to their converged values. With this in mind, initial conditions have been chosen which have more intuitive significance than $\bar{\lambda}$ and $\bar{\mu}$. The initial conditions chosen are presented in appendix C, along with the equations for calculating $\bar{\lambda}$ and $\bar{\mu}$ from these values. The rationale used for selecting initial guesses of the other unknown initial conditions is also presented in appendix C.

RESULTS AND DISCUSSION

The solution to the limited thrust attitude rate problem is most interesting in situations where a significant period at maximum rate is required. One area where this occurs is when the instantaneous impact point (IIP) constraints are factors in determining an acceptable trajectory. For launches from the Eastern Test Range (ETR), near polar orbits and hyperbolas with certain combinations of declination and right ascension of the outgoing asymptote require launch azimuths for planar trajectories which appear to be unacceptable because of the IIP traces. Dog-legged trajectories may be used to try to improve the traces by launching at a nonoptimum azimuth and constraining the thrust attitude to be parallel to the launch azimuth plane until some later time in the trajectory. Two cases were chosen to demonstrate that solutions could be obtained with the analysis described even though the eight-by-eight iteration required appears formidable. The procedures used to alter the IIP traces in the cases are examples of techniques which might be used to improve the traces. However, the traces presented do not necessarily satisfy range safety constraints.

The vehicle used in these demonstration cases is the Atlas-Centaur. The Atlas is propelled by two booster engines and one sustainer engine. The booster engines are jettisoned at a predetermined acceleration level. The sustainer engine continues to burn (sustainer solo). The Centaur insulation panels and then the payload fairing are jettisoned in this phase. The sustainer solo ends at propellant depletion and the Atlas stage

is jettisoned. After approximately 10 seconds, the Centaur engines ignite and burn continuously until the desired injection conditions are reached.

As mentioned in the section TRAJECTORY DESCRIPTION, the trajectories consist of a short vertical rise followed by a rapid pitchover phase determining the amount of trajectory lofting during the near zero angle-of-attack atmospheric phase. This near zero angle-of-attack phase lasts until the booster engines are jettisoned. Then the steering is determined by the variational solution.

The first mission is a sun-synchronous circular orbit at 1110 kilometers altitude. An inclination of 99.9° is required to take advantage of precession due to oblateness to maintain sun synchronization. A launch azimuth of about 193° would be required for a planar trajectory to the required orbit. Atlas-Centaur trajectories from ETR at that launch azimuth present severe, if not insurmountable, range safety problems because scheduled hardware drops (booster engines, insulation panels, payload fairing, Atlas stage) as well as the IIP trace endanger land areas. Hence, a launch azimuth of 108° was chosen for the demonstration trajectory to avoid these hardware impact problems. The thrust attitude is constrained to be parallel to the launch azimuth plane until 5 seconds after Centaur ignition (268 sec after lift-off) after which the attitude is unconstrained. The rate of change of attitude is constrained to be less than or equal to 1.6° per second. The free parameter during the atmospheric portion, the pitchover, is optimized. The thrust attitude from booster jettison to injection is optimized using the analysis and techniques described in this report. The IIP trace for this trajectory is presented in figure 1. A spherical earth model with no drag is used to calculate the IIP trace. The injected payload weight is 800 kilograms. A trajectory with the same ground rules, but with no attitude rate constraint, achieved an injected payload weight of 820 kilograms. Thus, the payload loss due to the attitude rate limit is 20 kilograms. The two IIP traces are virtually identical. The thrust attitude in pitch (ψ) and yaw (β) (see fig. 2) are presented in figures 3 and 4, respectively. The thrust attitude rate is discontinuously increased to the limiting rate of 1.6° per second 0.07 second before the thrust attitude is freed from the planar constraint and remains at that level for the following 34 seconds. Figures 3 and 4 show that during the planar portion of the trajectory the thrust vector is directed such that altitude is gained at the expense of horizontal velocity. It is the horizontal velocity which must be turned to satisfy the final inclination. After the planar constraint is removed, the thrust attitude rapidly approaches the horizontal to accumulate the required circular velocity. The total rate of change of thrust angle, altitude, inertial flight path angle, and velocity as functions of time are presented in figures 5, 6, 7, and 8, respectively.

Launch trajectories from ETR to sun-synchronous orbits unavoidably present range safety problems because the instantaneous impact point traces will always cross populated land areas in the Caribbean and/or South America. It is impossible to avoid over-

fly for any practical trajectory regardless of the method used to alter the IIP trace. The trajectory chosen in this report does not necessarily reflect the best choice from a range safety standpoint. It is used only to demonstrate an application of the analysis to a mission where significant attitude and attitude rate constraints are present.

The second demonstration case is characteristic of another range safety problem whereby the IIP trace can be moved to avoid all land masses. For certain combinations of declination and right ascension of the outgoing geocentric asymptote, planar interplanetary trajectories possess impact point traces which cross South America, in particular Venezeula and Brazil. It is possible in some of these cases to move the IIP trace north to avoid all land masses. This is demonstrated in the trace presented in figure 9. The declination and right ascension of the outgoing asymptote are -45° and 190.5° east of the launch site meridian, respectively. The injection energy is 4.0215 square kilometers per square second with a perigee altitude of 167 kilometers. The planar trajectory would require about a 200° launch azimuth. A planar trajectory at this launch azimuth would be unacceptable because the hardware impact points and IIP traces impinge land. However, land masses are completely avoided by choosing a launch azimuth of 108° and by constraining the thrust attitude to be parallel to the launch azimuth plane until 150 seconds after Centaur ignition. The rate of change of thrust attitude is again limited to 1.6° per second. The pitchover phase is optimum. The thrust attitude rate is increased discontinuously to the limiting value 0.4 second before the planar constraint is removed and continues at the maximum rate for the following 17 seconds. The injected payload weight for this case is about 227 kilograms. A similar trajectory without the attitude rate limit constraint achieved about a 2 kilogram increase in payload weight. Figures 10 to 15 show the thrust angles in pitch and yaw, the total rate of change of the thrust angle, the inertial flight path angle, and the velocity and altitude, respectively, as functions of time.

CONCLUDING REMARKS

The problem of obtaining the required terminal conditions for orbital and planetary missions while satisfying typical range safety constraints has been considered. To simplify the mathematical problem, a planar attitude constraint was imposed for the initial portion of the flight in order to avoid overflight of certain land areas. Later in flight, the attitude constraint is removed in order to allow the required terminal conditions to be achieved. An attitude rate limit is also imposed in order to prevent discontinuous attitude changes.

The mathematical problem is formulated by using the calculus of variations. Euler-Lagrange equations are obtained which determine the optimum thrust direction profile subject to the problem constraints. A simplified procedure is also presented for obtain-

ing the auxiliary variational boundary conditions required for free end conditions.

To illustrate the use of the equations, results are presented for two typical missions which require nonplanar trajectories of the type discussed. These missions are a sun-synchronous orbit and a typical interplanetary probe. An Atlas-Centaur launch vehicle is assumed, launched from the Eastern Test Range.

Lewis Research Center,
National Aeronautics and Space Administration,
Cleveland, Ohio, January 3, 1969,
128-31-30-02-22.

APPENDIX A

SYMBOLS

a	thrust acceleration, m/sec^2
b_j	constraint equations
$\bar{b}_j$	constraint equations
C	first integral of Euler-Lagrange equations
$d( )$	differential of ( )
E	Weierstrass excess function
e	eccentricity
F	defined in eq. (1b)
$\hat{f}$	thrust direction vector
G	Earth gravitational constant, m^3/sec^2
$\bar{G}$	gravity acceleration vector, m/sec^2
g	function of initial and final conditions to be minimized, sec
H	energy, m^2/sec^2
h	angular momentum, m^2/sec
I	orbital inclination, rad
J	functional to be minimized by variational methods, sec
m	mass, kg
$\hat{n}$	unit normal to attitude constraint plane
p	semilatus rectum, m
q_k	generalized state variables
r	radius, m
S	constant vector in eq. (B6)
s	sign $(\hat{f} \times \bar{\sigma}) \cdot \hat{n}$
t	time, sec
$\bar{v}$	velocity vector, m/sec
x_i	problem variables
$\bar{y}$	constant vector
$\hat{z}$	unit vector pointing at North Pole
α	arbitrary scalar
β	yaw attitude, deg
γ	Lagrange multiplier, sec
$\Delta( )$	jump discontinuity in variable
$\delta( )$	denotes linearized variable
$\bar{\epsilon}$	arbitrary vector
η	true anomaly, rad
θ_o	commanded attitude discontinuity, rad
$\hat{\theta}$	unit tangential vector
$\bar{\lambda}$	Lagrange multipliers, sec^2/m
$\bar{\mu}$	Lagrange multipliers, sec/m
ρ	Lagrange multiplier, sec
σ_{mag}	magnitude of $\hat{f} \times \bar{\sigma}$ at t_1, sec
$\bar{\sigma}$	Lagrange multipliers, sec
φ	angle from injection to outgoing asymptote, rad
ψ	pitch attitude, rad
ω_m	maximum rotation rate, rad/sec
$\bar{\omega}$	rotation vector, rad/sec

Subscripts:

A	asymptote
av	average value
d	desired
f	final
h	normal
I	injection
i	problem variables
p	perigee
r	radial
t	fixed time
θ	tangential
0	initial
1	start of regular planar arc
2	start of unconstrained phase
3	start of singular unconstrained arc
∞	hyperbolic excess

Superscripts:

$\cdot$	derivative with respect to time
*	finite, but allowable variation of the variable
$\hat{}$	unit vector
$\bar{}$	vector
+	evaluated after switching point
-	evaluated before switching point

APPENDIX B

EQUATIONS FOR PROBLEM SOLUTION

The variational portion of the trajectory is divided into four phases, as discussed earlier. These phases, along with the definition of switching times, are presented in table I.

The following equations must be integrated throughout the variational portion of the trajectory (eqs. (2a), (2b), (3a), and (3b)).

$$\left.\begin{aligned} \dot{\bar{v}} + \frac{Gm}{r^3}\bar{r} - a\hat{f} &= \bar{0} \\ \dot{\bar{r}} - \bar{v} &= \bar{0} \\ \dot{\bar{\lambda}} + \bar{\mu} &= \bar{0} \\ \dot{\bar{\mu}} - \frac{Gm}{r^3}\bar{\lambda} + 3\frac{Gm}{r^5}(\bar{\lambda}\cdot\bar{r})\bar{r} &= \bar{0} \end{aligned}\right\} \tag{B1}$$

These equations are linearized, and the linearized equations are also integrated throughout the trajectory in order to obtain the partial derivatives required for the Newton-Raphson iteration. The linearized equations obtained from equations (B1) are

$$\left.\begin{aligned} \delta\dot{\bar{v}} + \frac{Gm}{r^3}\delta\bar{r} - 3\frac{Gm}{r^5}(\bar{r}\cdot\delta\bar{r})\bar{r} - a\delta\hat{f} &= \bar{0} \\ \delta\dot{\bar{r}} - \delta\bar{v} &= \bar{0} \\ \delta\dot{\bar{\lambda}} + \delta\bar{\mu} &= \bar{0} \\ \delta\dot{\bar{\mu}} - \frac{Gm}{r^3}\delta\bar{\lambda} + 3\frac{Gm}{r^5}\left[(\bar{r}\cdot\delta\bar{r})\bar{\lambda} + (\delta\bar{\lambda}\cdot\bar{r})\bar{r} + (\bar{\lambda}\cdot\delta\bar{r})\bar{r} + (\bar{\lambda}\cdot\bar{r})\delta\bar{r}\right] - 15\frac{Gm}{r^7}(\bar{\lambda}\cdot\bar{r})(\bar{r}\cdot\delta\bar{r})\bar{r} &= \bar{0} \end{aligned}\right\} \tag{B2}$$

where δ is used to indicate a linearized variable. As noted in the Numerical Iteration section, $\hat{f}\times\bar{\sigma}$ is not required until phase 2. It will be shown later that a closed form solution is available for $\hat{f}\times\bar{\sigma}$ during phase 3. Also, $\hat{f}\times\bar{\sigma}$ is identically zero during phase 4. The differential equation for $\hat{f}$ must be integrated during phases 2 and 3, while

the singular solution is used during phases 1 and 4. The additional equations to be integrated are (from eqs. (2c) and (3c))

Phase 2

$$\left.\begin{aligned} \frac{d}{dt}(\hat{f}\times\bar{\sigma}) &= a\bar{\lambda}\times\hat{f} - \bar{\omega}\times(\bar{\sigma}\times\hat{f}) \\ \frac{d}{dt}\left[\delta(\hat{f}\times\bar{\sigma})\right] &= a\delta\bar{\lambda}\times\hat{f} + a\bar{\lambda}\times\delta\hat{f} - \bar{\omega}\times\delta(\bar{\sigma}\times\hat{f}) \\ \dot{\hat{f}} &= \bar{\omega}\times\hat{f} \\ \dot{\delta\hat{f}} &= \bar{\omega}\times\delta\hat{f} \end{aligned}\right\} \tag{B3}$$

where $\bar{\omega} = \omega_m \text{ sign } \left[(\hat{f}\times\bar{\sigma})\cdot\hat{n}\right]\hat{n}$ (eq. (9)).

Phase 3

$$\left.\begin{aligned} \dot{\hat{f}} &= \bar{\omega}\times\hat{f} \\ \dot{\delta\hat{f}} &= \bar{\omega}\times\delta\hat{f} + \delta\bar{\omega}\times\hat{f} \end{aligned}\right\} \tag{B4}$$

where (from eq. (8))

$$\bar{\omega} = \omega_m \frac{\hat{f}\times\bar{\sigma}}{|\hat{f}\times\bar{\sigma}|}$$

and

$$\delta\bar{\omega} = \omega_m\left[\frac{\delta(\hat{f}\times\bar{\sigma})}{|\hat{f}\times\bar{\sigma}|} - \frac{(\hat{f}\times\bar{\sigma})(\hat{f}\times\bar{\sigma})\cdot\delta(\hat{f}\times\bar{\sigma})}{|\hat{f}\times\bar{\sigma}|^3}\right]$$

During phase 3, $\hat{f}\times\bar{\sigma}$ can be calculated in closed form by using the fact that

$$\bar{\lambda}\times\bar{v} + \bar{\mu}\times\bar{r} - \hat{f}\times\bar{\sigma} = \overline{\text{constant}} \tag{B5}$$

Equation (B5) can be verified by differentiation and using equations (2), (3), and (10). Therefore, $\hat{f}\times\bar{\sigma}$ can be calculated from

$$\hat{f} \times \bar{\sigma} = \bar{\lambda} \times \bar{v} + \bar{\mu} \times \bar{r} - \bar{S} \tag{B6}$$

where

$$\bar{S} = (\bar{\lambda} \times \bar{v} + \bar{\mu} \times \bar{r} - \hat{f} \times \bar{\sigma})_{t_2} \tag{B7}$$

Taking the variations of equations (B6) and (B7) results in

$$\delta(\hat{f} \times \bar{\sigma}) = (\delta\bar{\lambda} \times \bar{v} + \bar{\lambda} \times \delta\bar{v} + \delta\bar{\mu} \times \bar{r} + \bar{\mu} \times \delta\bar{r} - \delta\bar{S}) \tag{B8}$$

and

$$\delta\bar{S} = \left[\delta\bar{\lambda} \times \bar{v} + \bar{\lambda} \times \delta\bar{v} + \delta\bar{\mu} \times \bar{r} + \bar{\mu} \times \delta\bar{r} - \delta(\hat{f} \times \bar{\sigma})\right]_{t_2} \tag{B9}$$

Calculation of Thrust Direction

During phase 1, the thrust direction is calculated from equation (14):

$$\hat{f} = \frac{\hat{\lambda} - (\hat{\lambda} \cdot \hat{n})\hat{n}}{\sqrt{1 - (\hat{\lambda} \cdot \hat{n})^2}} \tag{B10}$$

The variation of equation (B10) is

$$\delta\hat{f} = \frac{\delta\hat{\lambda} - (\delta\hat{\lambda} \cdot \hat{n})\hat{n}}{\sqrt{1 - (\hat{\lambda} \cdot \hat{n})^2}} + \frac{\left[\hat{\lambda} - (\hat{\lambda} \cdot \hat{n})\hat{n}\right](\hat{\lambda} \cdot \hat{n})(\delta\hat{\lambda} \cdot \hat{n})}{\left[1 - (\hat{\lambda} \cdot \hat{n})^2\right]^{3/2}} \tag{B11}$$

where

$$\delta\hat{\lambda} = \frac{\delta\bar{\lambda}}{\lambda} - \frac{\bar{\lambda}}{\lambda^3}(\delta\bar{\lambda} \cdot \bar{\lambda})$$

During phase 4, $\hat{f}$ is calculated from equation (12):

$$\hat{f} = \hat{\lambda}$$

and

$$\delta\hat{f} = \frac{\delta\bar{\lambda}}{\lambda} - \frac{\bar{\lambda}}{\lambda^3}(\delta\bar{\lambda} \cdot \bar{\lambda})$$

The thrust direction is integrated during phases 2 and 3, as indicated earlier.

Initial Conditions

The choice of initial conditions is discussed in appendix C, and the variable initial conditions are ψ, $\dot{\psi}$, β, $\dot{\beta}$, and $\dot{\lambda}$. In addition, the switching times t_1 and t_3 are used as variable initial conditions along with the value of σ_{mag} at t_1. Equations must be derived for the linearized changes in the initial values of $\bar{\lambda}$, $\bar{\mu}$, and $\hat{f} \times \bar{\sigma}$, obtained as a result of linearized changes in the variable initial conditions.

The initial variations in $\bar{\lambda}$ and $\bar{\mu}$ are obtained by linearizing equations (C5b) and (C5c):

$$\delta\bar{\lambda} = \lambda\delta\hat{\lambda}$$

$$\delta\bar{\mu} = -\lambda\delta\dot{\hat{\lambda}} - \delta\dot{\lambda}\hat{\lambda} - \dot{\lambda}\delta\hat{\lambda}$$

The initial value of λ is always equal to unity, and the initial values of $\hat{r}$, $\hat{\theta}$, and $\hat{h}$ are fixed because the initial position and velocity are specified. Also, the initial value of $\dot{\hat{r}}$ is fixed because $\dot{\hat{r}}$ is a function only of position and velocity and not thrust direction. Therefore, the variations of equations (C5a) and (C6) are

$$\delta\hat{\lambda} = \delta\lambda_r\hat{r} + \delta\lambda_\theta\hat{\theta} + \delta\lambda_h\hat{h}$$

and

$$\delta\dot{\hat{\lambda}} = \delta\dot{\lambda}_r\hat{r} + \delta\lambda_r\dot{\hat{r}} + \delta\dot{\lambda}_\theta\hat{\theta} + \delta\lambda_\theta\dot{\hat{\theta}} + \lambda_\theta\delta\dot{\hat{\theta}} + \delta\dot{\lambda}_h\hat{h} + \delta\lambda_h\dot{\hat{h}} + \lambda_h\delta\dot{\hat{h}}$$

Equations (C1), (C2), and (C3) are linearized to give

$$\delta\lambda_r = -\sin\beta\sin\psi\delta\beta + \cos\beta\cos\psi\delta\psi$$

$$\delta\lambda_\theta = -\sin\beta\cos\psi\delta\beta - \cos\beta\sin\psi\delta\psi$$

$$\delta\lambda_h = \cos\beta\delta\beta$$

$$\delta\dot{\lambda}_r = -\sin\beta\sin\psi\delta\dot{\beta} + \cos\beta\cos\psi\delta\dot{\psi} - (\dot{\beta}\cos\beta\sin\psi + \dot{\psi}\sin\beta\cos\psi)\delta\beta$$

$$-(\dot{\beta}\sin\beta\cos\psi + \dot{\psi}\cos\beta\sin\psi)\delta\psi$$

$$\delta\dot{\lambda}_\theta = -\sin\beta\cos\psi\delta\dot{\beta} - \cos\beta\sin\psi\delta\dot{\psi} - (\dot{\beta}\cos\beta\cos\psi - \dot{\psi}\sin\beta\sin\psi)\delta\beta$$

$$+(\dot{\beta}\sin\beta\sin\psi - \dot{\psi}\cos\beta\cos\psi)\delta\psi$$

$$\delta\dot{\lambda}_h = \cos\beta\delta\dot{\beta} - \dot{\beta}\sin\beta\delta\beta$$

$$\delta\dot{\hat{\theta}} = \frac{ar}{h}(\delta\hat{f}\cdot\hat{h})\hat{h}$$

$$\delta\dot{\hat{h}} = -\frac{ar}{h}(\delta\hat{f}\cdot\hat{h})\hat{h}$$

where $\delta\hat{f}$ is calculated by using equation (B11).

Some of the linearized variables have jump discontinuities at a definite time due to the allowable variation in this time. These jumps occur when the derivative of the variable is discontinuous at this time and are calculated from equations of the form

$$(\delta x)_t^+ = (\delta x)_t^- + \left(\dot{x}_t^+ - \dot{x}_t^-\right)\delta t \tag{B12}$$

where δx_t is the linearized change at fixed time and the minus and plus superscripts denote evaluation of the variable before and after t, respectively.

The derivative of $\hat{f}$ is discontinuous at t_1. The derivative after t_1 is given by equation (9).

$$(\dot{\hat{f}})_{t_1}^+ = \bar{\omega}\times\hat{f} = \omega_m\,\mathrm{sign}\left[(\hat{f}\times\bar{\sigma})\cdot\hat{n}\right]\hat{n}\times\hat{f}$$

and $(\dot{\hat{f}})_{t_1}^-$ is evaluated by differentiating equation (B10):

$$(\dot{\hat{f}})_{t_1}^- = \frac{\dot{\hat{\lambda}} - (\dot{\hat{\lambda}}\cdot\hat{n})\hat{n}}{\sqrt{1-(\hat{\lambda}\cdot\hat{n})^2}} + \frac{\left[\hat{\lambda} - (\hat{\lambda}\cdot\hat{n})\hat{n}\right](\hat{\lambda}\cdot\hat{n})(\dot{\hat{\lambda}}\cdot\hat{n})}{\left[1-(\hat{\lambda}\cdot\hat{n})^2\right]^{3/2}}$$

where

$$\dot{\hat{\lambda}} = \frac{\dot{\overline{\lambda}}}{\lambda} - \frac{\overline{\lambda}(\overline{\lambda} \cdot \dot{\overline{\lambda}})}{\lambda^3} = -\frac{\overline{\mu}}{\lambda} + \frac{\hat{\lambda}(\hat{\lambda} \cdot \overline{\mu})}{\lambda}$$

Therefore, by using equation (B12),

$$(\delta\hat{f})^+_{t_1} = (\delta\hat{f})^-_{t_1} + \left(\dot{\hat{f}}^+_{t_1} - \dot{\hat{f}}^-_{t_1}\right)\delta t_1$$

The derivative of $\hat{f} \times \overline{\sigma}$ is also discontinuous at t_1, but the situation is somewhat different than for $\hat{f}$, since $\hat{f} \times \overline{\sigma}$ is initialized at t_1. When $\hat{f} \times \overline{\sigma}$ is initialized at t_1, the value is (from eq. (27))

$$\hat{f} \times \overline{\sigma} = \sigma_{mag}(\hat{f} \times \hat{n})$$

The value of $\hat{f} \times \overline{\sigma}$ at a later time $(t_1 + \delta t_1)$ is obtained by using equations (2c), (3c), and (9).

$$\begin{aligned}(\hat{f} \times \overline{\sigma})_{(t_1 + \delta t_1)} &= \sigma_{mag}(\hat{f} \times \hat{n}) + \frac{d}{dt}(\hat{f} \times \overline{\sigma})\delta t_1 \\ &= \sigma_{mag}(\hat{f} \times \hat{n}) + a(\overline{\lambda} \times \hat{f})\delta t_1 - \overline{\omega} \times (\overline{\sigma} \times \hat{f})\delta t_1 \\ &= \sigma_{mag}(\hat{f} \times \hat{n}) + a(\overline{\lambda} \times \hat{f})\delta t_1 + \sigma_{mag}\omega_m s\hat{n} \times (\hat{f} \times \hat{n})\delta t_1 \end{aligned} \qquad \text{(B12)}$$

where

$$s = \text{sign}(\hat{f} \times \overline{\sigma}) \cdot \hat{n}$$

When $\hat{f} \times \overline{\sigma}$ is initialized at a later time $(t_1 + \delta t_1)$, the value is

$$(\hat{f} \times \overline{\sigma})_{(t_1 + \delta t_1)} = \sigma_{mag}(\hat{f} \times \hat{n})_{(t_1 + \delta t_1)}$$

where, by using equations (2c) and (9)

$$\begin{aligned}(\hat{f} \times \hat{n})_{(t_1 + \delta t_1)} &= (\hat{f} \times \hat{n})_{t_1} + (\overline{\omega} \times \hat{f}) \times \hat{n}\delta t_1 \\ &= (\hat{f} \times \hat{n})_{t_1} + \omega_m s(\hat{n} \times \hat{f}) \times \hat{n}\delta t_1\end{aligned}$$

Then $\hat{f} \times \bar{\sigma}$ becomes

$$(\hat{f} \times \bar{\sigma})_{(t_1 + \delta t_1)} = \sigma_{mag}(\hat{f} \times \hat{n}) + \sigma_{mag}\omega_m s(\hat{n} \times \hat{f}) \times \hat{n}\delta t_1 \tag{B13}$$

The jump discontinuity in $\hat{f} \times \bar{\sigma}$ is given by the difference between equations (B13) and (B12):

$$\Delta(\hat{f} \times \bar{\sigma}) = -a(\bar{\lambda} \times \hat{f})\delta t_1$$

and the variation of $\hat{f} \times \bar{\sigma}$ at t_1 is given by

$$\delta(\hat{f} \times \bar{\sigma}) = \delta\sigma_{mag}(\hat{f} \times \hat{n}) + \sigma_{mag}(\delta\hat{f} \times \hat{n}) - a(\bar{\lambda} \times \hat{f})\delta t_1$$

During the iteration, the value of $\hat{f}$ is allowed to be discontinuous at t_3. This results in a jump discontinuity in $\delta\bar{v}$. The total $\delta\bar{v}$ is given by

$$(\delta\bar{v})^+_{t_3} = (\delta\bar{v})^-_{t_3} + a(\hat{f} - \hat{\lambda})^-_{t_3}\,\delta t_3$$

Final Conditions

The variational final conditions for the sun-synchronous mission are (see eq. (27)).

$$(\hat{f} \times \bar{\sigma})_{t_3} = \bar{0}$$

$$(\hat{f} \cdot \hat{\lambda})_{t_3} = 1$$

$$(\bar{\lambda} \times \bar{v} + \bar{\mu} \times \bar{r})_{t_f} \cdot \hat{z} = 0$$

$$\left[(\bar{\lambda} \times \bar{v} + \bar{\mu} \times \bar{r}) \cdot \bar{h}\right]_{t_f} = 0$$

For the interplanetary mission, the variational final conditions are

$$(\hat{f} \times \bar{\sigma})_{t_3} = \bar{0}$$

$$(\hat{f} \cdot \hat{\lambda})_{t_3} = 1$$

$$(\bar{\lambda} \cdot \bar{G} + \bar{\mu} \cdot \bar{v})_{t_f} = 0$$

$$(\bar{\lambda} \times \bar{v} + \bar{\mu} \times \bar{r}) \cdot \hat{v}_{\infty_{t_f}} = 0$$

In addition, there are three final conditions on state variables for both of the missions (energy is used for termination of the trajectory). The final state variable end conditions for the planetary mission are

(1) Perigee radius

(2) Declination of outgoing asymptote

(3) Right ascension of outgoing asymptote

Conditions 2 and 3 are equivalent to specified $\hat{v}_\infty$. For the sun-synchronous mission, the state variable end conditions are

(1) Radius

(2) Radius rate

(3) Inclination

In order for the iteration to converge on these final conditions, the linearized changes in final conditions are required. The changes in the variational end conditions at t_3 are obtained by using equations (2c), (3a), (10), and (B12).

$$\left[\delta(\hat{f} \times \bar{\sigma})\right]_{t_3}^{+} = \left[\delta(\hat{f} \times \bar{\sigma})\right]_{t_3}^{-} - a\left[(\bar{\lambda} \times \hat{f})\right]_{t_3}^{-} \delta t_3$$

$$\left[\delta(\hat{\lambda} \cdot \hat{f})\right]_{t_3}^{+} = \left[\delta(\hat{\lambda} \cdot \hat{f})\right]_{t_3}^{-} - \left[-\frac{\bar{\mu} \cdot \hat{f}}{\lambda} + \frac{(\hat{\lambda} \cdot \hat{f})\hat{\lambda}}{\lambda} + \hat{\lambda} \cdot (\bar{\omega} \times \hat{f})\right]_{t_3}^{-} \delta t_3$$

where $\bar{\omega}$ is evaluated by using equation (8). The changes in the variational final conditions at t_f are

$$\left.\begin{aligned} \delta(\bar{\lambda} \cdot \bar{G} + \bar{\mu} \cdot \bar{v})_{t_f} &= \left[\delta\bar{\lambda} \cdot \bar{G} - \frac{Gm}{r^3}\bar{\lambda} \cdot \delta\bar{r} + 3\frac{Gm}{r^5}(\bar{\lambda} \cdot \bar{r})(\bar{r} \cdot \delta\bar{r}) + \delta\bar{\mu} \cdot \bar{v} + \bar{\mu} \cdot \delta\bar{v}\right]_{t_f} \\ \delta\left[(\bar{\lambda} \times \bar{v} + \bar{\mu} \times \bar{r}) \cdot \bar{x}\right]_{t_f} &= \left[\delta\bar{\lambda} \times \bar{v} + \bar{\lambda} \times \delta\bar{v} + \bar{\mu} \times \delta\bar{r} + \delta\bar{\mu} \times \bar{r})\right]_{t_f} \cdot \bar{x}_{t_f} + (\bar{\lambda} \times \bar{v} + \bar{\mu} \times \bar{r})_{t_f} \cdot \delta\bar{x} \end{aligned}\right\} \quad \text{(B14)}$$

The $\delta\bar{r}$, $\delta\bar{v}$, $\delta\bar{\lambda}$, and $\delta\bar{\mu}$ at t_f in the preceding equations have been modified to be variations at constant energy rather than constant time. The following equations are used to modify these variables:

$$\delta t_f = -\frac{\delta H}{\dot{H}} = -\left[\frac{\bar{v}\cdot\delta\bar{v} + \frac{Gm}{r^3}\bar{r}\cdot\delta\bar{r}}{a\hat{\lambda}\cdot\bar{v}}\right]_{t_f}$$

$$\delta\bar{r} = (\delta\bar{r})_{t_f} + \bar{v}_{t_f}\delta t_f$$

$$\delta\bar{v} = (\delta\bar{v})_{t_f} + \left(a\hat{\lambda} - \frac{Gm}{r^3}\bar{r}\right)_{t_f}\delta t_f$$

$$\delta\bar{\lambda} = (\delta\bar{\lambda})_{t_f} - \bar{\mu}_{t_f}\delta t_f$$

$$\delta\bar{\mu} = (\delta\bar{\mu})_{t_f} + \dot{\bar{\mu}}_{t_f}\delta t_f$$

where H is the injection energy

$$H = \frac{\bar{v}\cdot\bar{v}}{2} - \frac{Gm}{r}$$

The $\delta\bar{x}$ in the last of equations (B14) is zero if $\bar{x}$ is $\bar{v}_\infty$ or $\hat{z}$. If $\bar{x}$ corresponds to $\bar{h}$, then

$$\delta\bar{x} = \delta\bar{h} = (\delta\bar{r}\times\bar{v} + \bar{r}\times\delta\bar{v})_{t_f}$$

In order to determine the linearized changes in final state conditions, these final conditions must first be expressed in terms of $\bar{r}$ and $\bar{v}$. The perigee radius is expressed as follows:

$$r_p = \frac{p}{1+e}$$

where

$$p = \frac{h^2}{Gm} = \frac{(\bar{r} \times \bar{v}) \cdot (\bar{r} \times \bar{v})}{Gm}$$

and

$$e = \sqrt{1 + \frac{2Hh^2}{(Gm)^2}}$$

The direction of the outgoing asymptote is given by

$$\hat{v}_\infty = \hat{r} \cos \varphi + \hat{\theta} \sin \varphi$$

(see sketch b), where $\varphi = \eta_A - \eta_I$ and the true anomalies are given by (ref. 7)

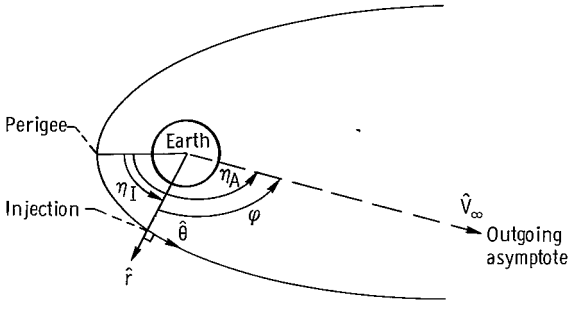

(b)

$$\eta_A = \cos^{-1}\left(-\frac{1}{e}\right)$$

$$\eta_I = \sin^{-1}\left(\sqrt{\frac{p}{Gm}}\,\frac{\bar{r} \cdot \bar{v}}{er}\right)$$

The radius rate and inclination (for the sun-synchronous mission) may be calculated from

$$\dot{r} = \hat{r} \cdot \bar{v}$$

$$I = \cos^{-1}\left(\frac{\bar{h} \cdot \hat{z}}{h}\right)$$

The linearized changes in the state variable end conditions are then given by

$$\delta r_p = 2\frac{(\bar{h} \cdot \delta\bar{h})}{h^2} r_p \left(1 - \frac{r_p H}{Gme}\right)$$

$$\delta\bar{v}_\infty = \delta\hat{r} \cos\varphi + \delta\hat{\theta} \sin\varphi + (\hat{\theta} \cos\varphi - \hat{r} \sin\varphi)\delta\varphi$$

where

$$\delta\hat{r} = \frac{\delta\bar{r}}{r} - \frac{(\bar{r} \cdot \delta\bar{r})}{r^3}\bar{r}$$

$$\delta\hat{h} = \frac{\delta\bar{h}}{h} - \frac{(\bar{h} \cdot \delta\bar{h})\bar{h}}{h^3}$$

$$\delta\hat{\theta} = \delta\hat{h} \times \hat{r} + \hat{h} \times \delta\hat{r}$$

$$\delta\varphi = \delta\eta_A - \delta\eta_I$$

$$\delta\eta_A = -\frac{2H\bar{h} \cdot \delta\bar{h}}{(Gm)^2 e^2 \sqrt{e^2 - 1}}$$

$$\delta\eta_I = \tan\eta_I \left[\frac{\bar{h} \cdot \delta\bar{h}}{Gmp} + \frac{\delta\bar{r} \cdot \bar{v} + \bar{r} \cdot \delta\bar{v}}{\bar{r} \cdot \bar{v}} - \frac{2H\bar{h} \cdot \delta\bar{h}}{(Gm)^2 e^2} - \frac{\bar{r} \cdot d\bar{r}}{r^2}\right]$$

The linearized changes in $\dot{r}$ and I are given by

$$\delta\dot{r} = \delta\hat{r} \cdot \bar{v} + \hat{r} \cdot \delta\bar{v}$$

$$\delta I = -\frac{\delta\hat{h} \cdot \hat{z}}{\sin I}$$

APPENDIX C

CHOICE OF INITIAL CONDITIONS

Solution of the two point boundary value problem requires initial guesses for eight variables, six of which are Lagrange multipliers. These variables are listed in equation (27). In order to eliminate the difficulty in guessing at values of these multipliers, equations are derived which express four of the multipliers in terms of pitch and yaw attitude and rate. In addition, equations are presented for deriving reasonable first guesses of the other multipliers and switching times.

The pitch attitude ψ and yaw attitude β are defined in figure 2. If the attitude were not constrained to be planar, the vehicle attitude would be along the $\hat{\lambda}$ vector. Therefore, the guesses of ψ, $\dot{\psi}$, β, and $\dot{\beta}$ correspond to the optimum values for the unconstrained attitude case. The coordinate axes in figure 2 correspond to a unit radial, tangential, normal coordinate system defined by

$$\left.\begin{aligned} r &= \frac{\bar{r}}{r} \\ h &= \frac{\bar{r} \times \bar{v}}{|\bar{r} \times \bar{v}|} \\ \hat{\theta} &= \hat{h} \times \hat{r} \end{aligned}\right\} \tag{C1}$$

The following equations are easily obtained from the figure:

$$\left.\begin{aligned} \lambda_r &= \hat{\lambda} \cdot \hat{r} = \cos\beta \sin\psi \\ \lambda_\theta &= \hat{\lambda} \cdot \hat{\theta} = \cos\beta \cos\psi \\ \lambda_h &= \hat{\lambda} \cdot \hat{h} = \sin\beta \end{aligned}\right\} \tag{C2}$$

Equations (C2) are differentiated to give

$$\left.\begin{aligned} \dot{\lambda}_r &= -\dot{\beta} \sin\beta \sin\psi + \dot{\psi} \cos\beta \cos\psi \\ \dot{\lambda}_\theta &= -\dot{\beta} \sin\beta \cos\psi - \dot{\psi} \cos\beta \sin\psi \\ \dot{\lambda}_h &= \dot{\beta} \cos\beta \end{aligned}\right\} \tag{C3}$$

The coordinate system defined in equations (C1) is not inertial. The derivatives of equations (C1) are given by

$$\left.\begin{aligned} \dot{\hat{r}} &= \frac{h}{r^2}\hat{\theta} \\ \dot{\hat{\theta}} &= \frac{ar}{h}\lambda_h\hat{h} - \frac{h}{r^2}\hat{r} \\ \dot{\hat{h}} &= -\frac{ar}{h}\lambda_h\hat{\theta} \end{aligned}\right\} \tag{C4}$$

where

$$h = |\bar{r} \times \bar{v}|$$

The values of $\bar{\lambda}$ and $\bar{\mu}$ can now be calculated from

$$\left.\begin{aligned} \hat{\lambda} &= \lambda_r\hat{r} + \lambda_\theta\hat{\theta} + \lambda_h\hat{h} \\ \bar{\lambda} &= \lambda\hat{\lambda} \\ \bar{\mu} &= -\dot{\bar{\lambda}} = -\lambda\dot{\hat{\lambda}} - \dot{\lambda}\hat{\lambda} \end{aligned}\right\} \tag{C5}$$

where $\dot{\hat{\lambda}}$ is calculated from equations (C3) and (C4) by using

$$\dot{\hat{\lambda}} = \dot{\lambda}_r\hat{r} + \dot{\lambda}_\theta\hat{\theta} + \dot{\lambda}_h\hat{h} + \lambda_r\dot{\hat{r}} + \lambda_\theta\dot{\hat{\theta}} + \lambda_h\dot{\hat{h}} \tag{C6}$$

It remains to supply values for λ and $\dot{\lambda}$ in order to completely determine $\bar{\lambda}$ and $\bar{\mu}$. Recalling that the Euler Lagrange equations are homogeneous in the multipliers, λ can be set equal to unity without loss of generality. In order to estimate $\dot{\lambda}$, it is first noted that if there is no planar attitude constraint, the vector

$$\bar{\lambda} \times \bar{v} + \bar{\mu} \times \bar{r} + \bar{\sigma} \times \hat{f} \tag{C7}$$

is a constant of the motion. This can easily be verified by differentiating and using equations (2) and (3). Both of the missions discussed herein contain required final conditions of the form

$$(\bar{\lambda} \times \bar{v} + \bar{\mu} \times \bar{r}) \cdot \bar{y} = 0 \tag{C8}$$

(see eq. (20) and (22)) where $\bar{y}$ is some fixed vector ($\hat{z}$ or $\bar{v}_\infty$). Also, if the initial and final attitudes are not specified, $\bar{\sigma} \times \hat{f} = \bar{0}$ at the beginning and end of the variational problem. Therefore, under these restricted conditions, equation (C8) can be satisfied at the beginning of the trajectory, thus reducing the iteration size. Equation (C8) is satisfied by the proper choice of the initial value of $\dot{\lambda}$. Combining equations (C5) and (C8) results in

$$\dot{\lambda} = \lambda \frac{(\hat{\lambda} \times \bar{v} - \dot{\hat{\lambda}} \times \bar{r}) \cdot \bar{y}}{(\hat{\lambda} \times \bar{r}) \cdot \bar{y}} \tag{C9}$$

Because of the attitude constraint during part of the trajectory, the vector in equation (C7) is not constant throughout the trajectory. Therefore, equation (C9) is not exact and the iteration size cannot be reduced. However, equation (C9) still supplies a reasonable first guess for $\dot{\lambda}$.

A reasonable guess for t_3 may be obtained by estimating the angular discontinuity at t_2 for the nonrate-limited case and dividing by the maximum vehicle turning rate:

$$t_3 = t_2 + \frac{\cos^{-1}(\hat{\lambda} \cdot \hat{f})_{t_2}}{\omega_m}$$

The value of t_1 is more difficult to estimate, but $(t_2 - t_1)$ should generally be an order of magnitude smaller than $(t_3 - t_2)$.

An additional multiplier remains to be estimated, which is the value of σ_{mag} in the equation

$$(\hat{f} \times \bar{\sigma})_{t_1} = \sigma_{mag}(\hat{f} \times \hat{n})_{t_1}$$

The estimating procedure for σ_{mag} starts by noting that

$$|\hat{f} \times \bar{\sigma}|_{t_1} = (\sigma_{mag})_{t_1}$$

and $|\hat{f} \times \bar{\sigma}|$ must be zero at t_3. Also,

$$\frac{d}{dt}(\hat{f} \times \bar{\sigma}) = -a\hat{f} \times \bar{\lambda}$$

between t_2 and t_3. Since the time interval (t_1, t_2) is much shorter than (t_2, t_3), σ_{mag} may be estimated as

$$\sigma_{mag} \approx - \int_{t_2}^{t_3} \frac{d}{dt} \left| \hat{f} \times \bar{\sigma} \right| \, dt \tag{C10}$$

During the interval (t_2, t_3), the motion of $\hat{f}$ is essentially toward $\bar{\lambda}$, while $\bar{\lambda}$ remains nearly constant. Therefore, the direction of $\hat{f} \times \bar{\lambda}$ is essentially fixed, so that

$$\frac{d}{dt} \left| \hat{f} \times \bar{\sigma} \right| \approx -a \left| \hat{f} \times \bar{\lambda} \right|$$

and

$$\sigma_{mag} \approx \int_{t_2}^{t_3} a \left| \hat{f} \times \bar{\lambda} \right| \, dt$$

The value of λ in this integral may be assumed to be unity, since $\lambda = 1$ at t_o and $\dot{\lambda}$ is very small. If a is assumed constant (equal to its average value), σ_{mag} becomes

$$\sigma_{mag} \approx \int_0^{t_3 - t_2} a \sin (\theta_o - \omega_m t) \, dt \approx \frac{a_{av}}{\omega_m} (1 - \cos \theta_o) \tag{C11}$$

where

$$\cos \theta_o = (\hat{\lambda} \cdot \hat{f})_{t_2}$$

and a_{av} is the average acceleration between t_2 and t_3.

REFERENCES

1. Teren, Fred; and Spurlock, Omer F.: Payload Optimization of Multistage Launch Vehicles. NASA TN D-3191, 1966.

2. MacKay, John S.; and Rossa, Leonard G.: A Variational Method for the Optimization of Interplanetary Round-Trip Trajectories. NASA TN D-1660, 1963.

3. Johnson, G. W.; and Winfield, D. H.: On a Singular Control Problem in Optimal Rocket Guidance. Paper 67-582, AIAA, Aug. 1967.

4. Bliss, Gilbert A.: Lectures on the Calculus of Variations. Univ. Chicago Press, 1946.

5. Leitmann, G.: On a Class of Variational Problems in Rocket Flight. J. Aero/Space Sci., vol. 26, no. 9, Sept. 1959, pp. 586-591.

6. Spurlock, Omer F.; and Teren, Fred: A Trajectory Code for Maximizing the Payload of Multistage Launch Vehicles. NASA TN D-4729, 1968.

7. Dobson, Wilbur F.; Huff, Vearl N.; and Zimmerman, Arthur V.: Elements and Parameters of the Osculating Orbit and Their Derivatives. NASA TN D-1106, 1962.

TABLE I. - TRAJECTORY PHASES AND SWITCHING TIMES

Event time	Description	Sun-synchronous trajectory	Interplanetary trajectory
		Time of occurrence, sec	
Liftoff	Vertical rise	0	0
	Pitchover and near-zero angle of attack booster trajectory	20	20
t_0	Start of singular planar arc (phase 1)	156.00	155.27
t_1	Start of regular planar arc (phase 2)	267.73	405.44
t_2	Start of regular unconstrained arc (phase 3)	267.80	405.86
t_3	Start of singular unconstrained arc (phase 4)	301.76	422.45
t_f	Powered flight termination	706.54	710.06

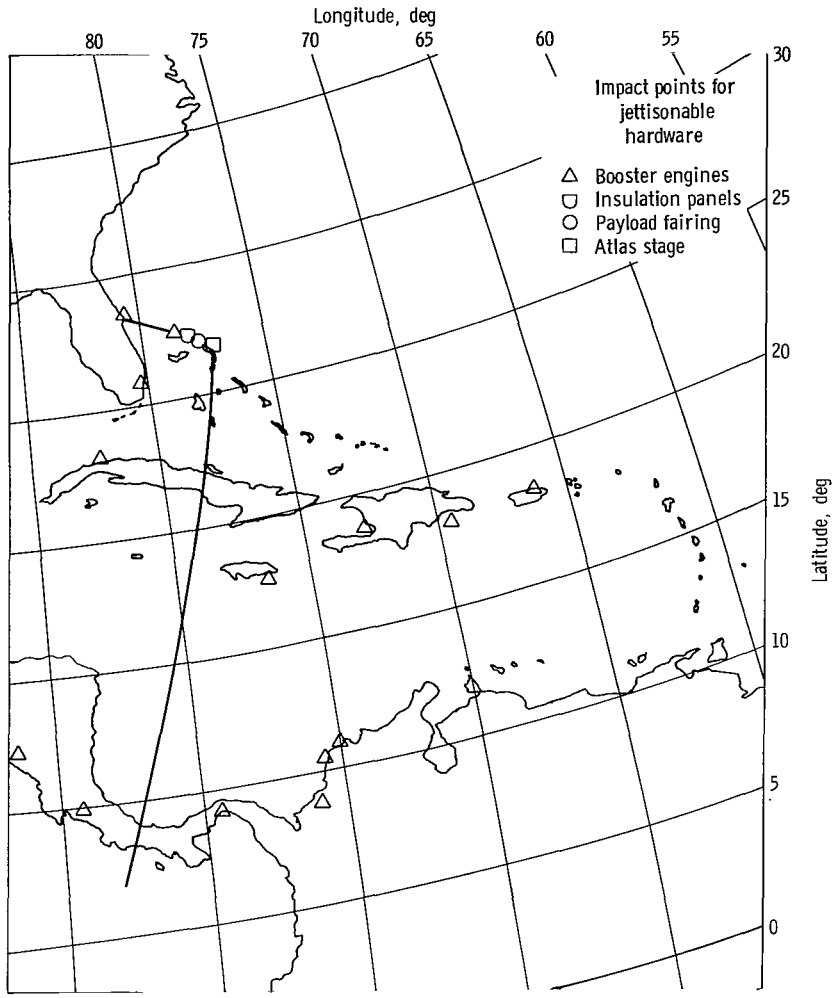

Figure 1. - Instantaneous impact point trace. Sun-synchronous trajectory

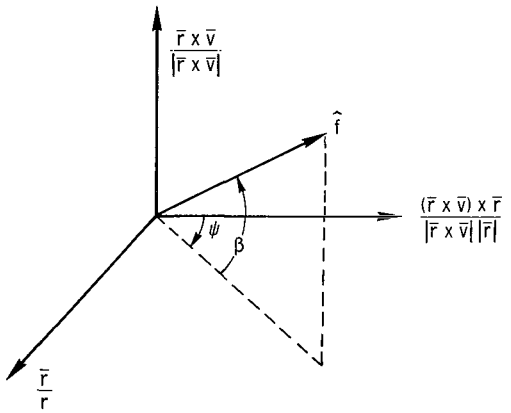

Figure 2. - Vehicle pitch and yaw attitudes.

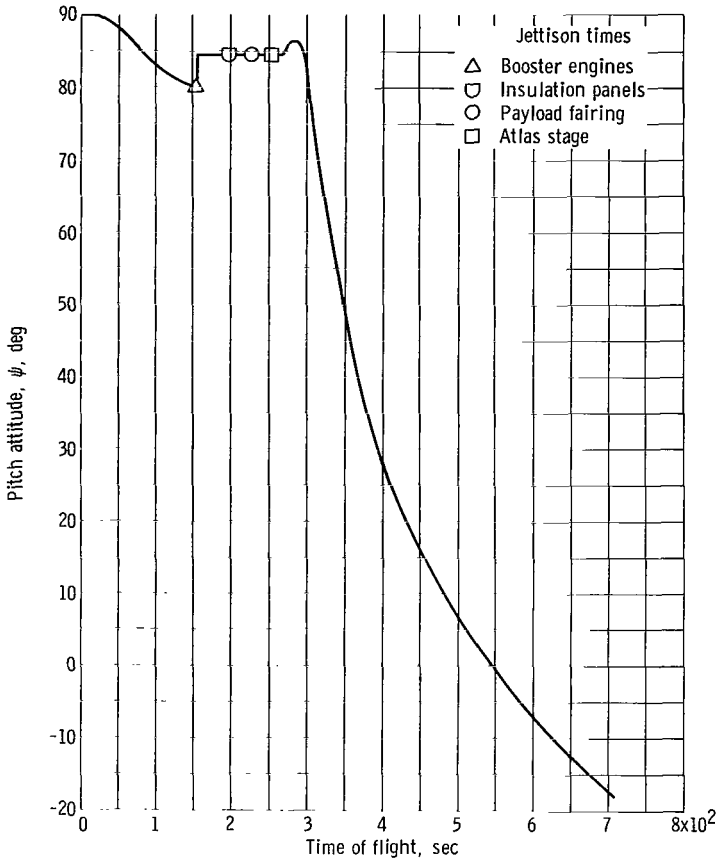

Figure 3. - Vehicle pitch attitude as function of time. Sun-synchronous trajectory.

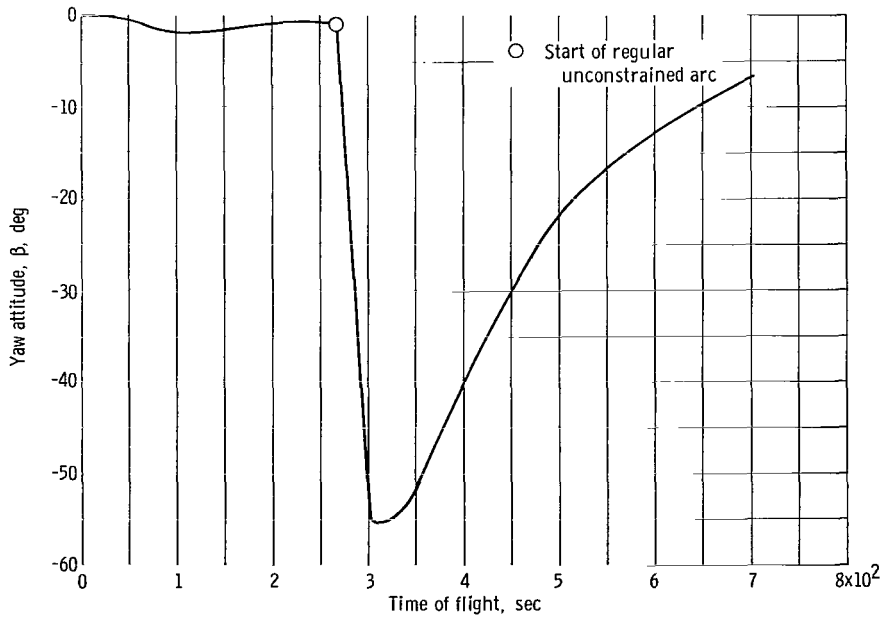

Figure 4. - Vehicle yaw attitude as function of time. Sun-synchronous trajectory.

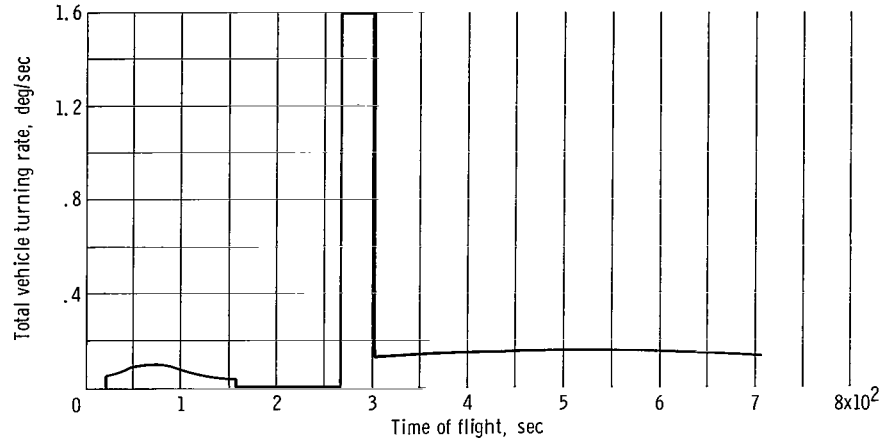

Figure 5. - Total vehicle turning rate as function of time. Sun-synchronous trajectory.

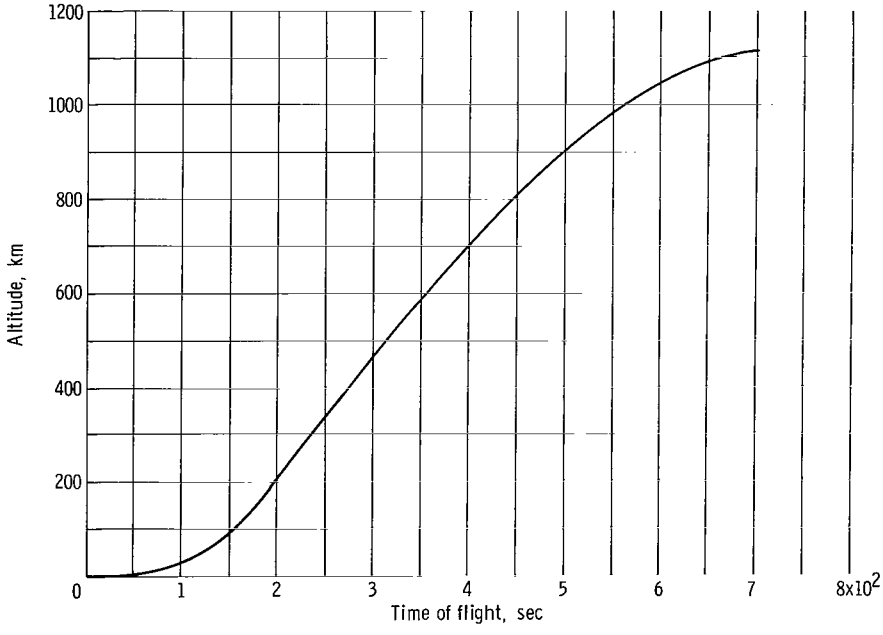

Figure 6. - Altitude as function of time. Sun-synchronous trajectory.

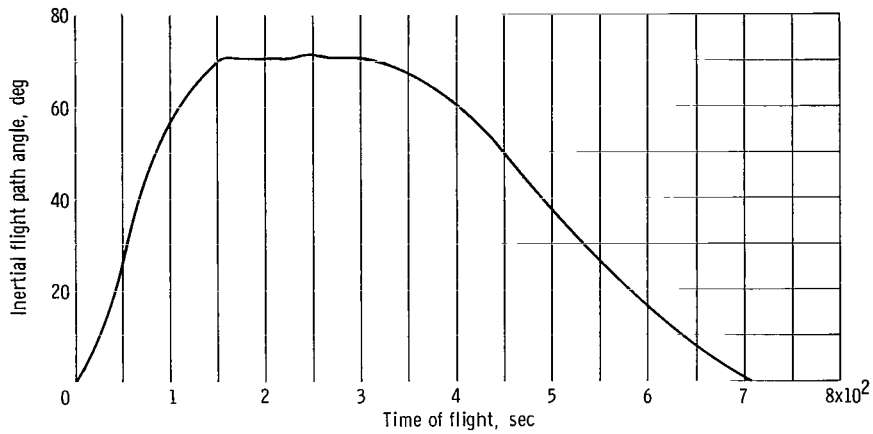

Figure 7. - Inertial flight path angle as function of time. Sun-synchronous trajectory.

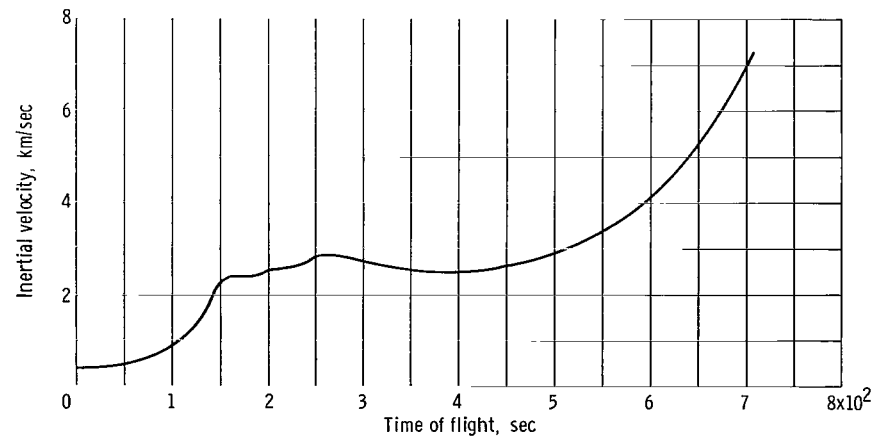

Figure 8. - Inertial velocity as function of time. Sun-synchronous trajectory.

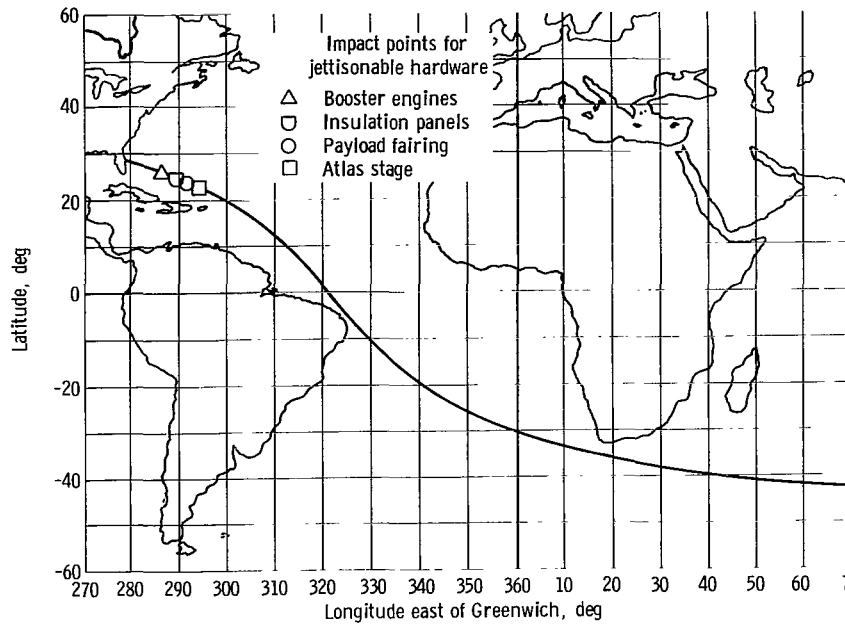

Figure 9. - Instantaneous impact point trace. Interplanetary trajectory.

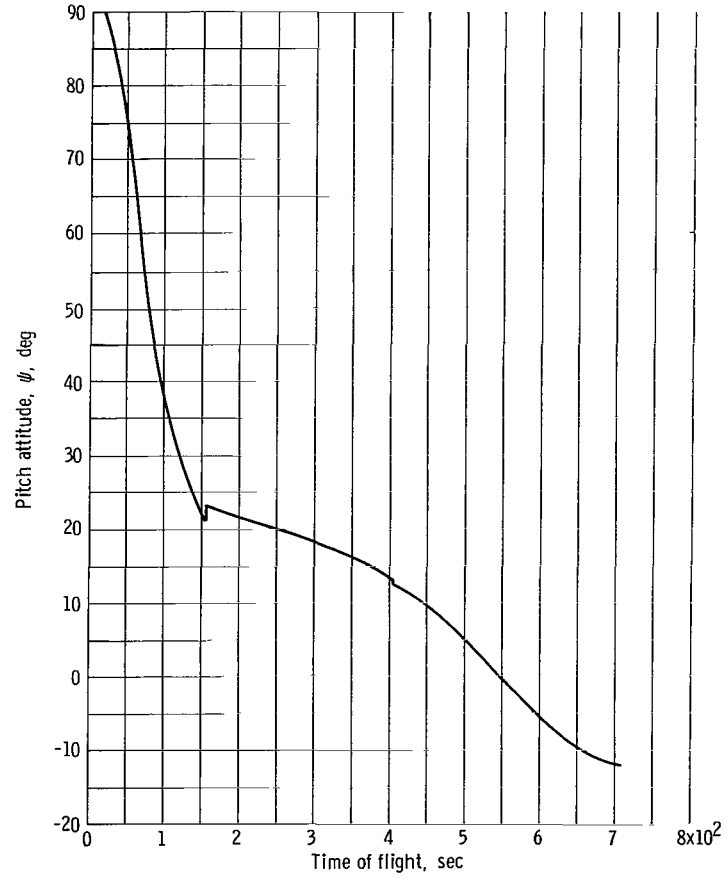

Figure 10. - Vehicle pitch attitude as function of time. Interplanetary trajectory.

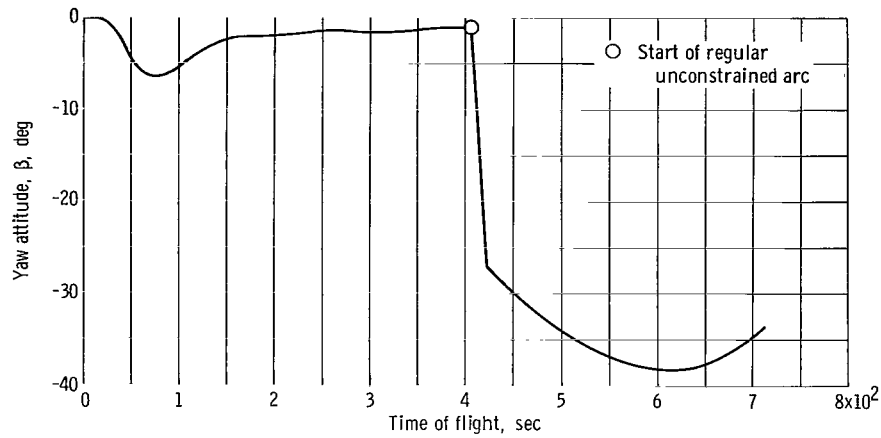

Figure 11. - Vehicle yaw attitude as function of time. Interplanetary trajectory.

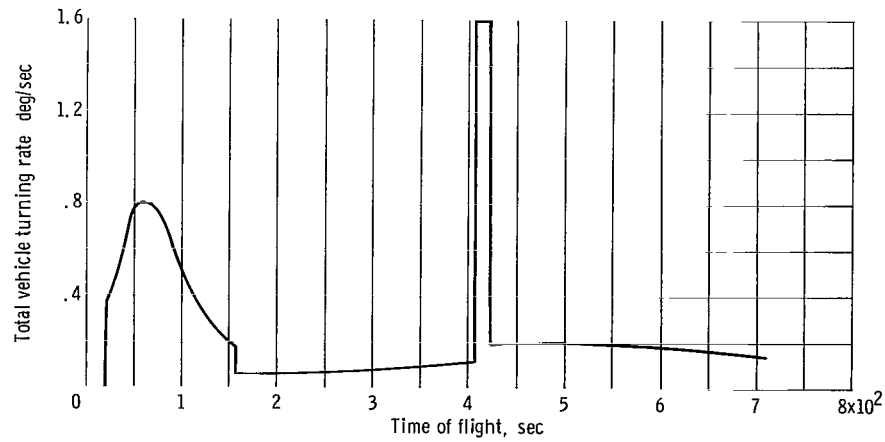

Figure 12. - Total vehicle turning rate as function of time. Interplanetary trajectory.

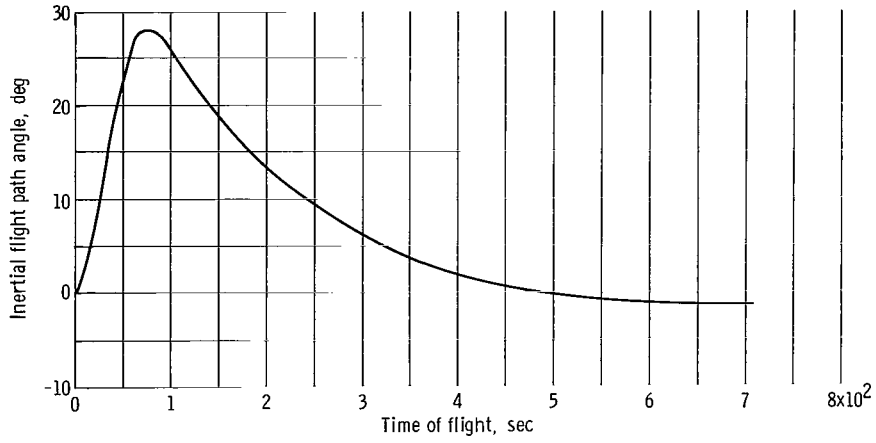

Figure 13. - Inertial flight path angle as function of time. Interplanetary trajectory.

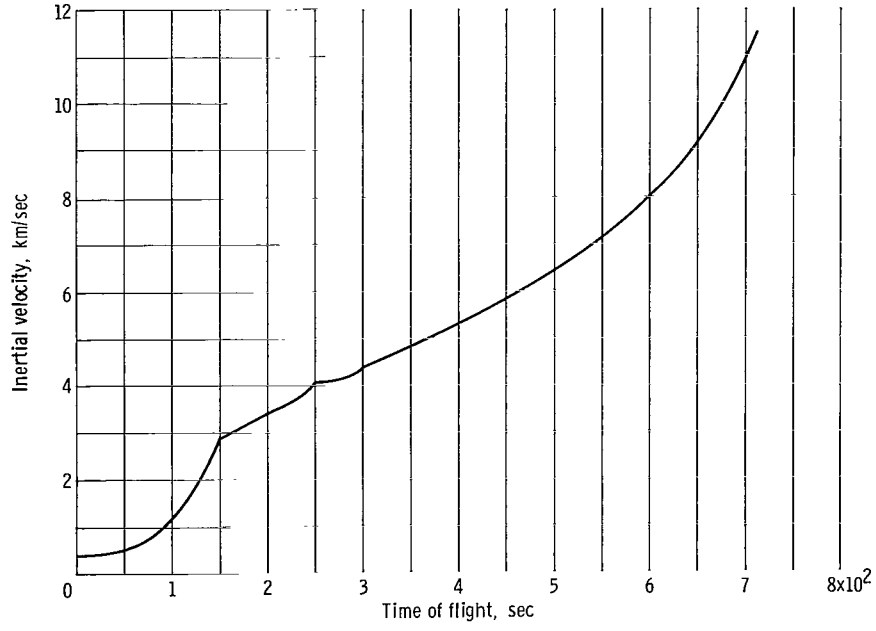

Figure 14. - Inertial velocity as function of time. Interplanetary trajectory.

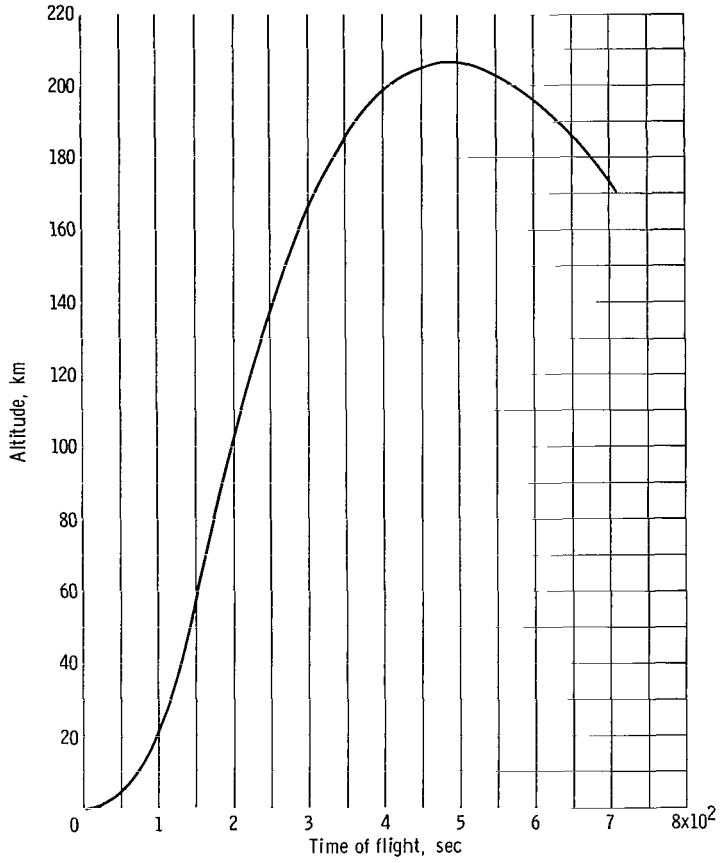

Figure 15. - Altitude as function of time. Interplanetary trajectory.

"The aeronautical and space activities of the United States shall be conducted so as to contribute . . . to the expansion of human knowledge of phenomena in the atmosphere and space. The Administration shall provide for the widest practicable and appropriate dissemination of information concerning its activities and the results thereof."

—NATIONAL AERONAUTICS AND SPACE ACT OF 1958

NASA SCIENTIFIC AND TECHNICAL PUBLICATIONS

TECHNICAL REPORTS: Scientific and technical information considered important, complete, and a lasting contribution to existing knowledge.

TECHNICAL NOTES: Information less broad in scope but nevertheless of importance as a contribution to existing knowledge.

TECHNICAL MEMORANDUMS: Information receiving limited distribution because of preliminary data, security classification, or other reasons.

CONTRACTOR REPORTS: Scientific and technical information generated under a NASA contract or grant and considered an important contribution to existing knowledge.

TECHNICAL TRANSLATIONS: Information published in a foreign language considered to merit NASA distribution in English.

SPECIAL PUBLICATIONS: Information derived from or of value to NASA activities. Publications include conference proceedings, monographs, data compilations, handbooks, sourcebooks, and special bibliographies.

TECHNOLOGY UTILIZATION PUBLICATIONS: Information on technology used by NASA that may be of particular interest in commercial and other non-aerospace applications. Publications include Tech Briefs, Technology Utilization Reports and Notes, and Technology Surveys.

Details on the availability of these publications may be obtained from:

SCIENTIFIC AND TECHNICAL INFORMATION DIVISION

NATIONAL AERONAUTICS AND SPACE ADMINISTRATION

Washington, D.C. 20546